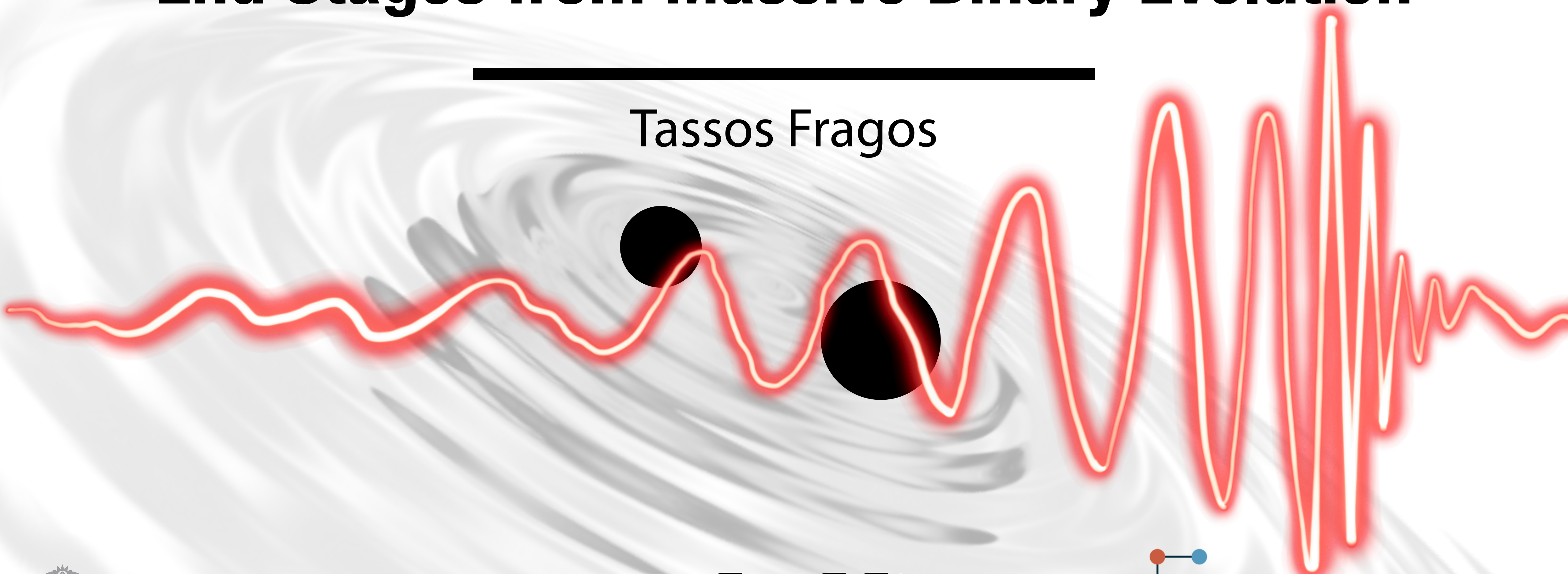


End Stages from Massive Binary Evolution

Tassos Fragos



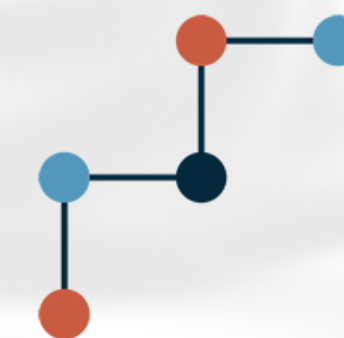
**UNIVERSITÉ
DE GENÈVE**

FACULTÉ DES SCIENCES
Département d'astronomie



GWSC

GRAVITATIONAL
WAVE
SCIENCE
CENTER



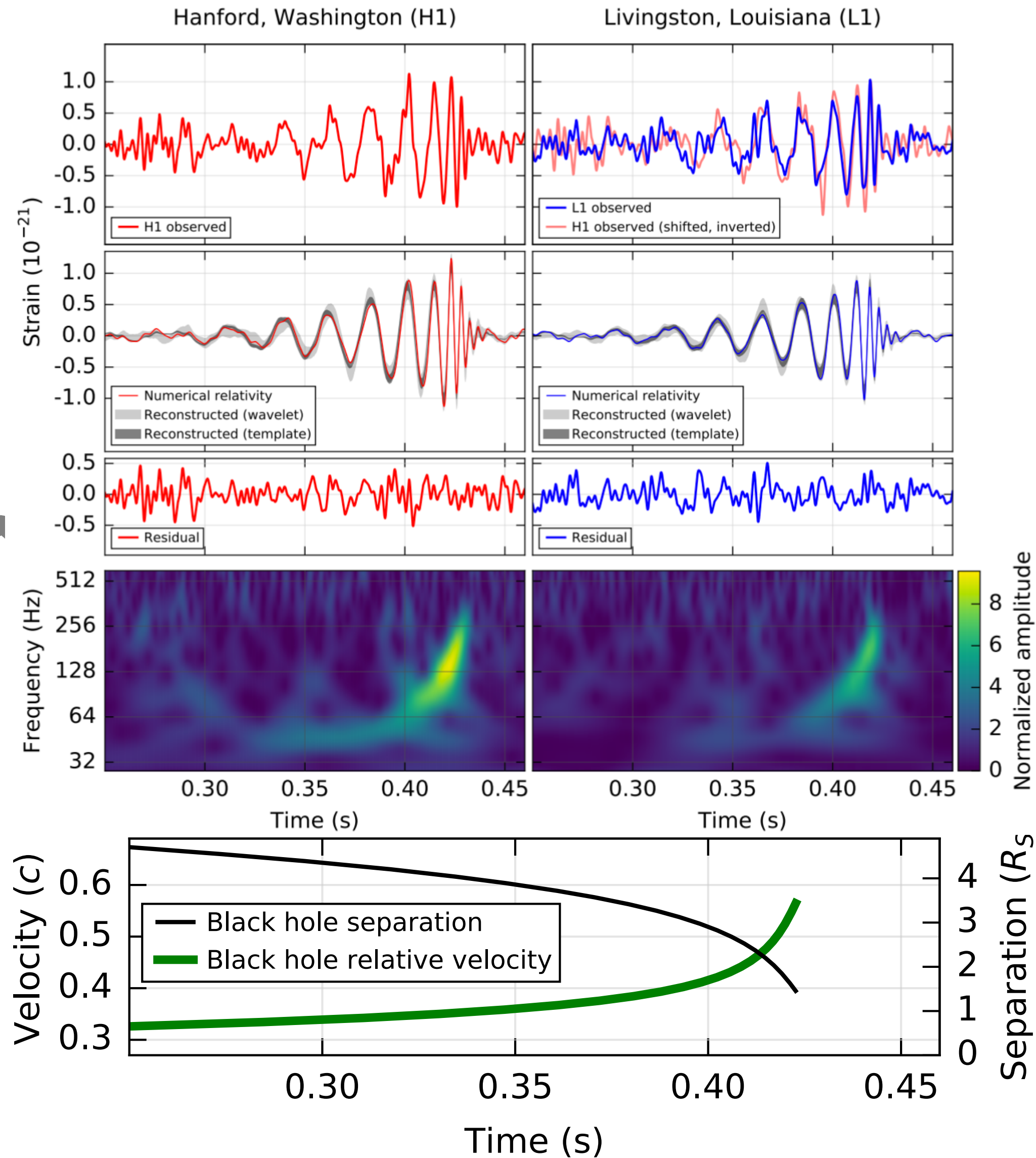
**Swiss National
Science Foundation**

30th Anniversary of the Rencontres du Vietnam - Windows on the Universe

Quy Nhon, 09/08/2023

The detection of the first gravitational-wave event

LIGO+VIRGO collaboration (2016) - arXiv:1602.03837



Detection with **5-sigma** confidence.
This means that the rate at which a signal analogous to GW150914 is created by noise is less than 1 in every 203,000 years.

3 solar masses of energy is what was released in gravitational waves.

10 times more luminous than all the stars of the Universe!!!

The detection of the first gravitational-wave event

LIGO+VIRGO collaboration (2016) - arXiv:1602.03840

	EOBNR	IMRPhenom	Overall
Detector-frame total mass M/M_{\odot}	$70.3^{+5.3}_{-4.8}$	$70.7^{+3.8}_{-4.0}$	$70.5^{+4.6\pm 0.9}_{-4.5\pm 1.0}$
Detector-frame chirp mass \mathcal{M}/M_{\odot}	$30.2^{+2.5}_{-1.9}$	$30.5^{+1.7}_{-1.8}$	$30.3^{+2.1\pm 0.4}_{-1.9\pm 0.4}$
Detector-frame primary mass m_1/M_{\odot}	$39.4^{+5.5}_{-4.9}$	$38.3^{+5.5}_{-3.5}$	$38.8^{+5.6\pm 0.9}_{-4.1\pm 0.3}$
Detector-frame secondary mass m_2/M_{\odot}	$30.9^{+4.8}_{-4.4}$	$32.2^{+3.6}_{-5.0}$	$31.6^{+4.2\pm 0.1}_{-4.9\pm 0.6}$
Detector-frame final mass M_f/M_{\odot}	$67.1^{+4.6}_{-4.4}$	$67.4^{+3.4}_{-3.6}$	$67.3^{+4.1\pm 0.8}_{-4.0\pm 0.9}$
Source-frame total mass $M^{\text{source}}/M_{\odot}$	$65.0^{+5.0}_{-4.4}$	$64.6^{+4.1}_{-3.5}$	$64.8^{+4.6\pm 1.0}_{-3.9\pm 0.5}$
Source-frame chirp mass $\mathcal{M}^{\text{source}}/M_{\odot}$	$27.9^{+2.3}_{-1.8}$	$27.9^{+1.8}_{-1.6}$	$27.9^{+2.1\pm 0.4}_{-1.7\pm 0.2}$
Source-frame primary mass $m_1^{\text{source}}/M_{\odot}$	$36.3^{+5.3}_{-4.5}$	$35.1^{+5.2}_{-3.3}$	$35.7^{+5.4\pm 1.1}_{-3.8\pm 0.0}$
Source-frame secondary mass $m_2^{\text{source}}/M_{\odot}$	$28.6^{+4.4}_{-4.2}$	$29.5^{+3.3}_{-4.5}$	$29.1^{+3.8\pm 0.2}_{-4.4\pm 0.5}$
Source-frame final mass $M_f^{\text{source}}/M_{\odot}$	$62.0^{+4.4}_{-4.0}$	$61.6^{+3.7}_{-3.1}$	$61.8^{+4.2\pm 0.9}_{-3.5\pm 0.4}$
Mass ratio q	$0.79^{+0.18}_{-0.19}$	$0.84^{+0.14}_{-0.21}$	$0.82^{+0.16\pm 0.01}_{-0.21\pm 0.03}$
Effective inspiral spin parameter χ_{eff}	$-0.09^{+0.19}_{-0.17}$	$-0.03^{+0.14}_{-0.15}$	$-0.06^{+0.17\pm 0.01}_{-0.18\pm 0.07}$
Dimensionless primary spin magnitude a_1	$0.32^{+0.45}_{-0.28}$	$0.31^{+0.51}_{-0.27}$	$0.31^{+0.48\pm 0.04}_{-0.28\pm 0.01}$
Dimensionless secondary spin magnitude a_2	$0.57^{+0.40}_{-0.51}$	$0.39^{+0.50}_{-0.34}$	$0.46^{+0.48\pm 0.07}_{-0.42\pm 0.01}$
Final spin a_f	$0.67^{+0.06}_{-0.08}$	$0.67^{+0.05}_{-0.05}$	$0.67^{+0.05\pm 0.00}_{-0.07\pm 0.03}$
Luminosity distance D_L/Mpc	390^{+170}_{-180}	440^{+140}_{-180}	$410^{+160\pm 20}_{-180\pm 40}$
Source redshift z	$0.083^{+0.033}_{-0.036}$	$0.093^{+0.028}_{-0.036}$	$0.088^{+0.031\pm 0.004}_{-0.038\pm 0.009}$
Upper bound on primary spin magnitude a_1	0.65	0.71	0.69 ± 0.05
Upper bound on secondary spin magnitude a_2	0.93	0.81	0.88 ± 0.10
Lower bound on mass ratio q	0.64	0.67	0.65 ± 0.03
Log Bayes factor $\ln \mathcal{B}_{\text{s/n}}$	288.7 ± 0.2	290.1 ± 0.2	—

$$\text{Chirp mass: } M_{\text{chirp}} = \frac{(m_1 m_2)^{3/5}}{(m_1 + m_2)^{1/5}}$$

$$\text{Effective spin parameter: } \chi_{\text{eff}} = \frac{m_1 \mathbf{a}_1 + m_2 \mathbf{a}_2}{m_1 + m_2} \hat{\mathbf{L}}$$

$$\text{Mass ratio: } q = \frac{m_2}{m_1}$$

Luminosity Distance: D_L
or
redshift of merger: z_{merger}

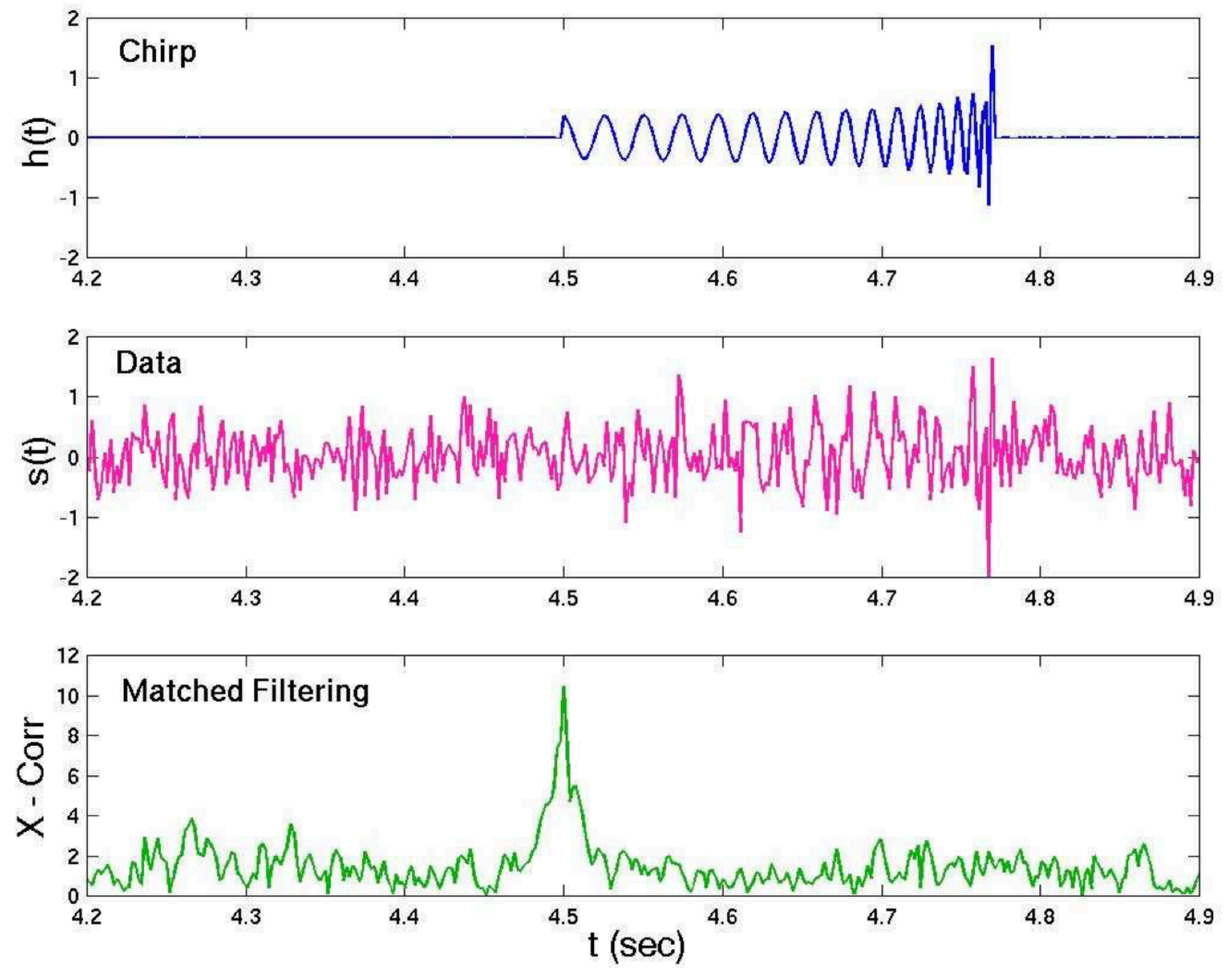
LIGO+VIRGO collaboration (2016) - arXiv:1602.03846

The detection confirms that:

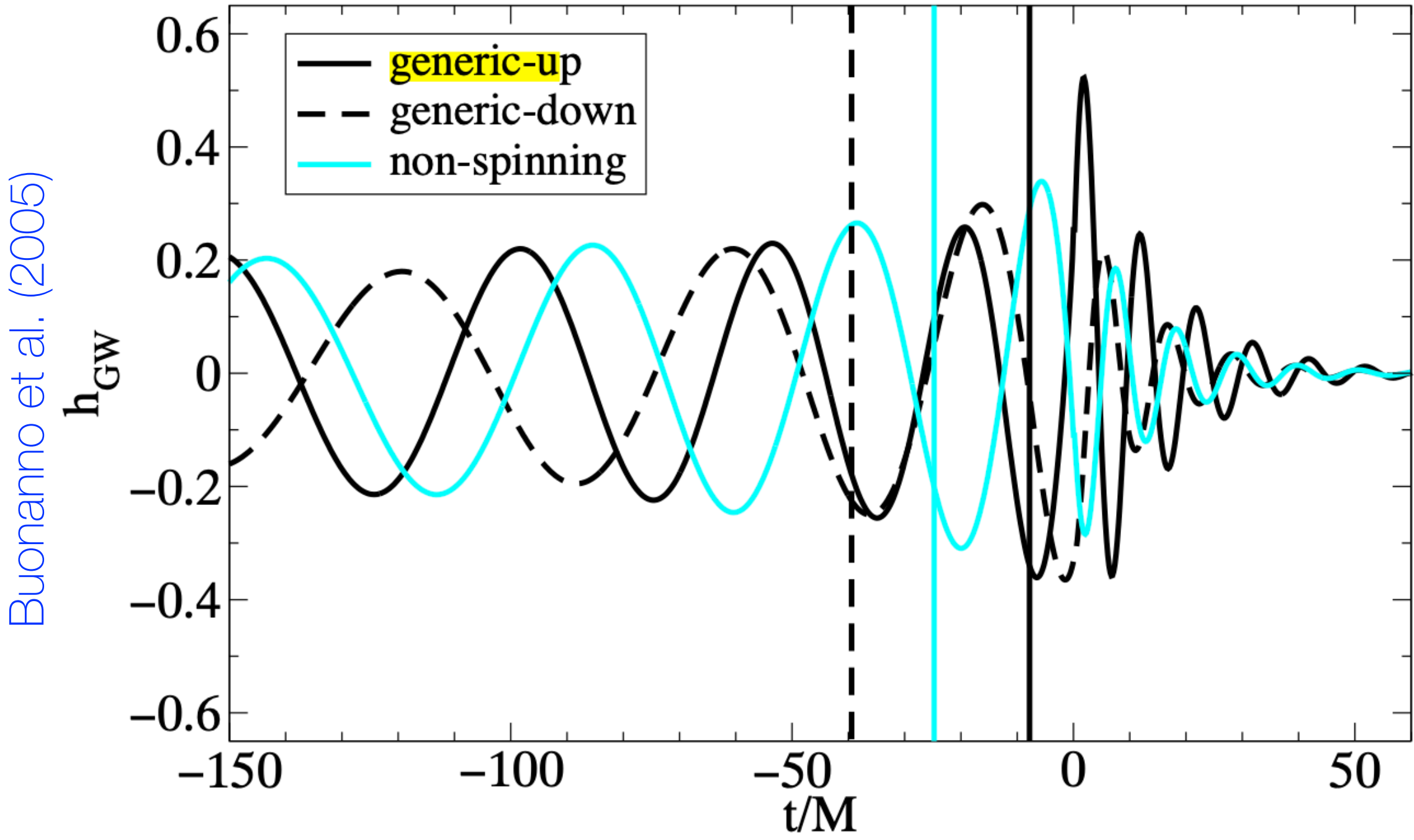
- 1) “heavy” black holes (BHs) exist
- 2) binary BHs form in nature
- 3) Binary BHs merge within a Hubble time (at a detectable rate)

The matched filtering technique

16-dimensional (9 intrinsic + 7 extrinsic) waveform template banks



Dhurandhar et al (2004)



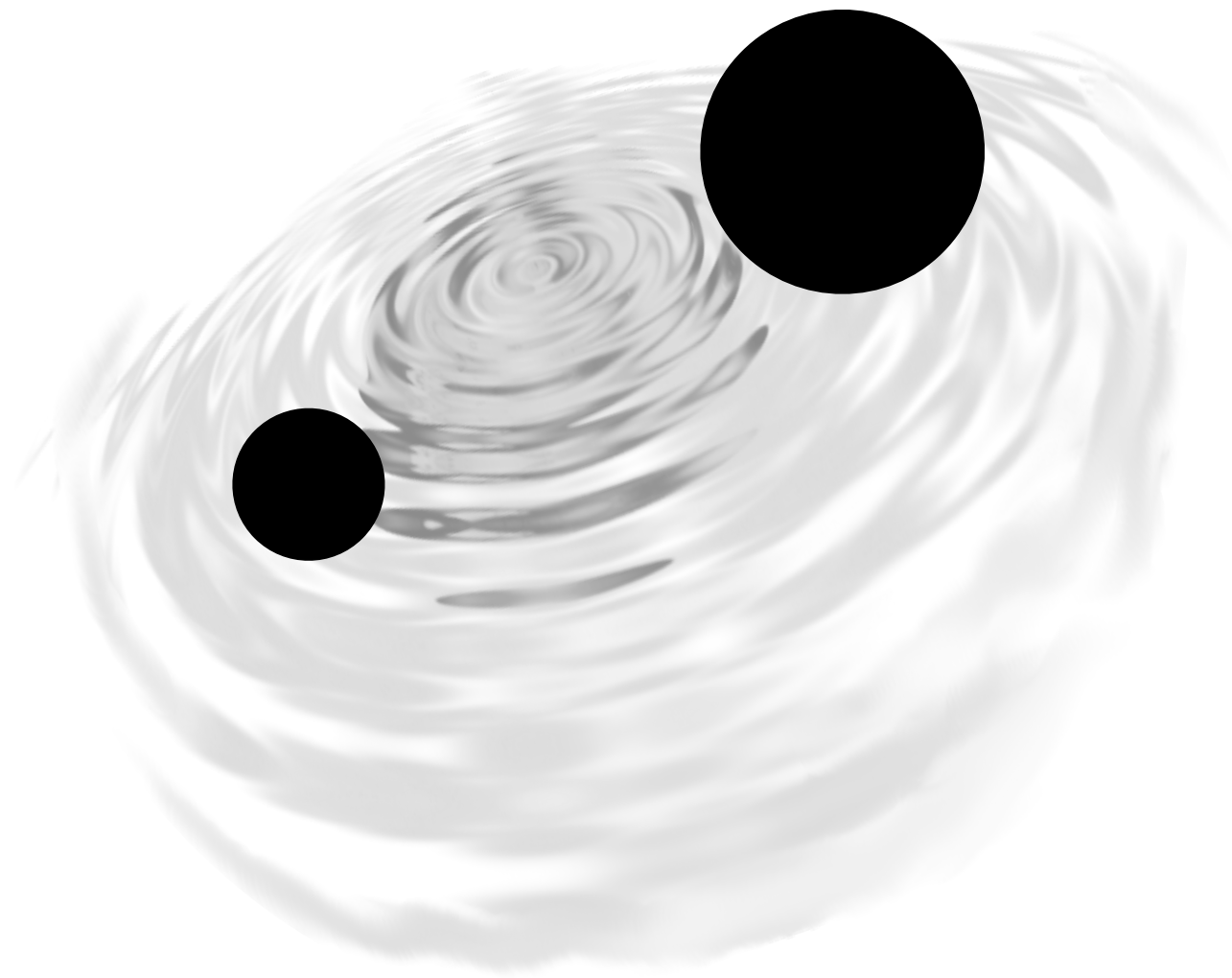
Buonanno et al. (2005)

Scaling of characteristic strain:
$$h \sim 2.5 \times 10^{-23} \left(\frac{\mathcal{M}}{\mathcal{M}_\odot} \right)^{5/3} \left(\frac{r}{100 \text{ Mpc}} \right)^{-1} \left(\frac{f}{100 \text{ Hz}} \right)^{2/3}$$

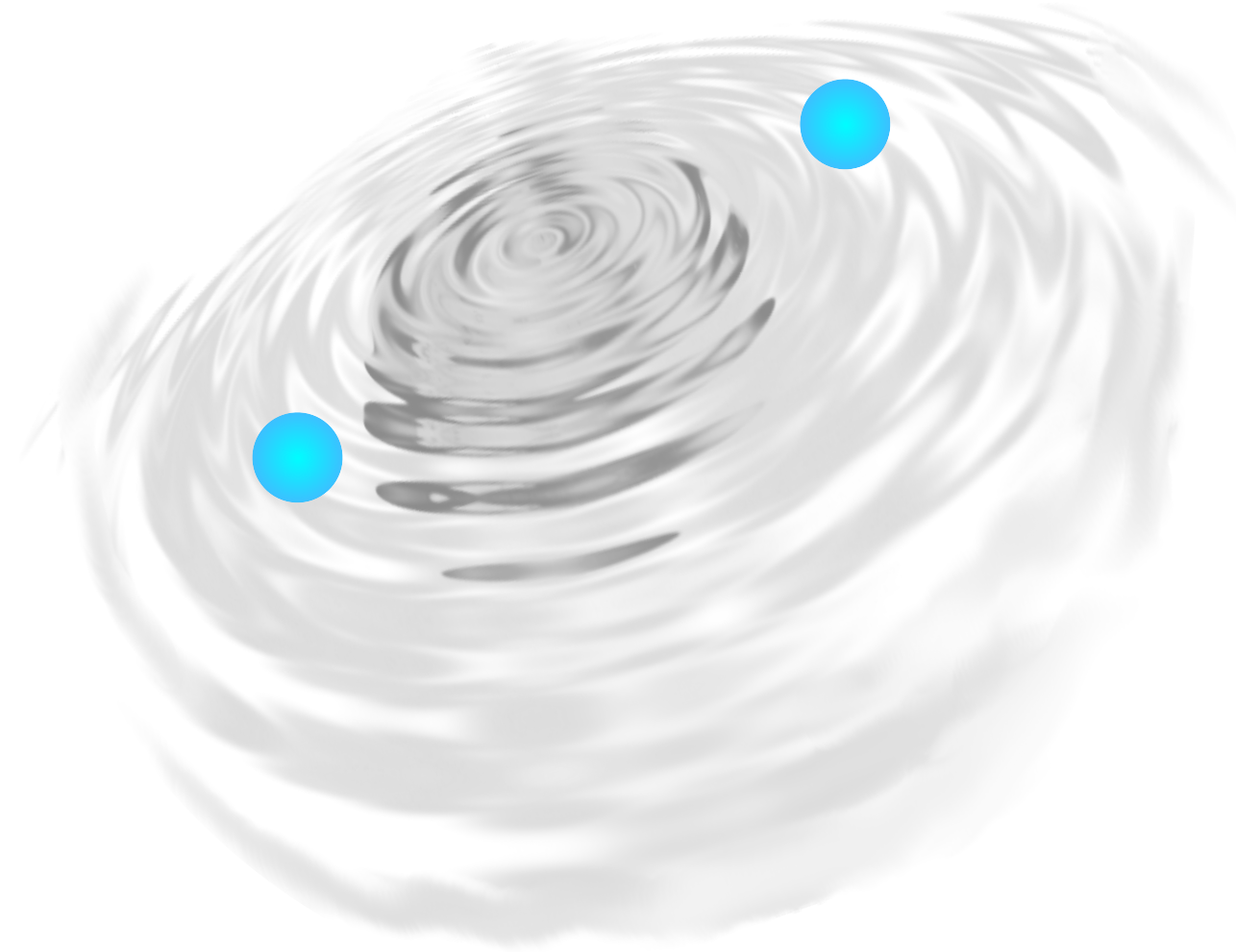
A $30M_\odot$ BH is ~32 more likely to be observed than a $15M_\odot$ one,
 while a $60M_\odot$ is ~1024 more likely to be observed than a $15M_\odot$ one!!!

The Gravitational-Wave Transient Catalogue 3 (GWTC-3)

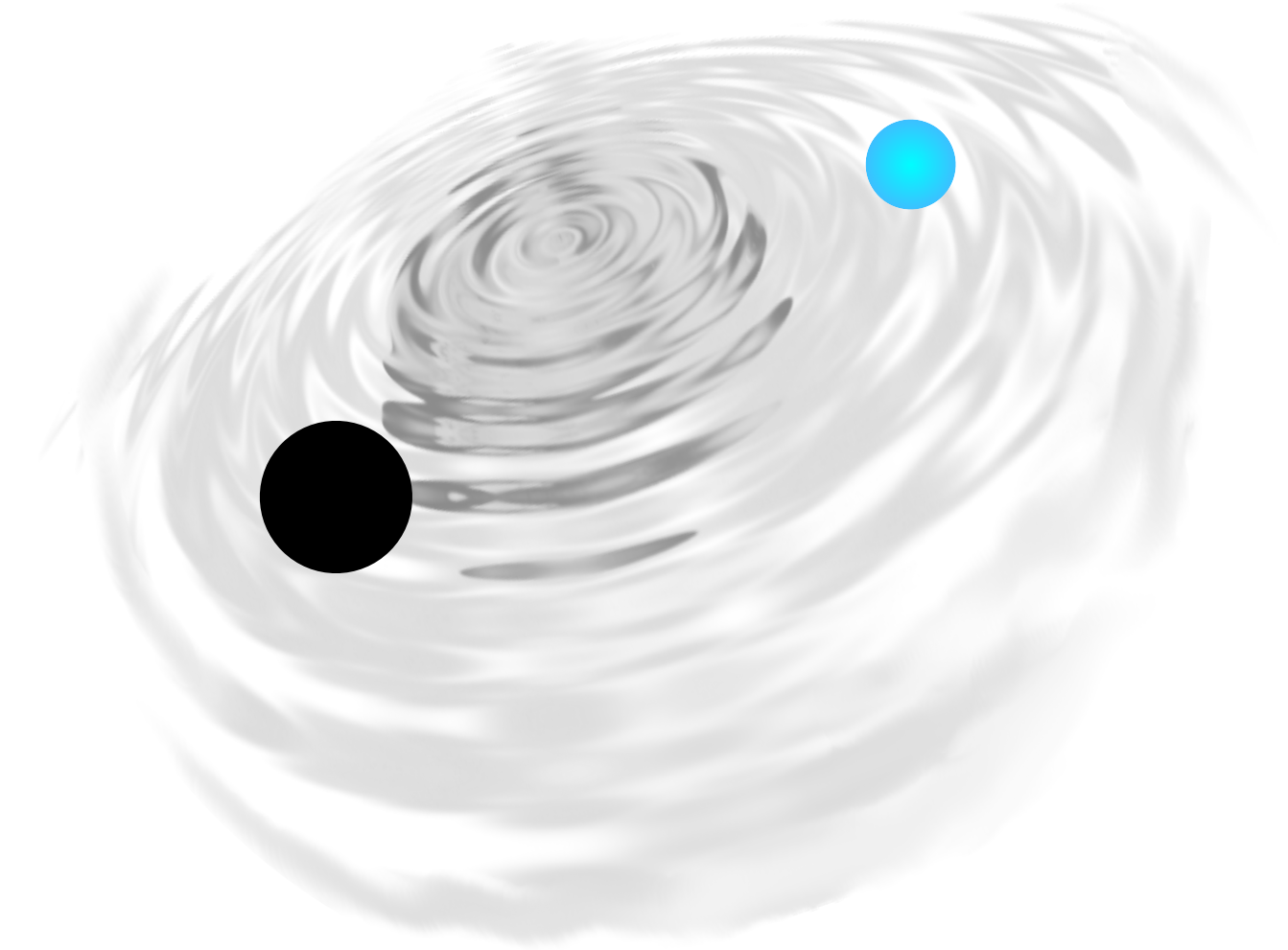
Abbot et al. [arXiv:2111.03606](https://arxiv.org/abs/2111.03606) (2021)



83-85
binary black holes (BBH)



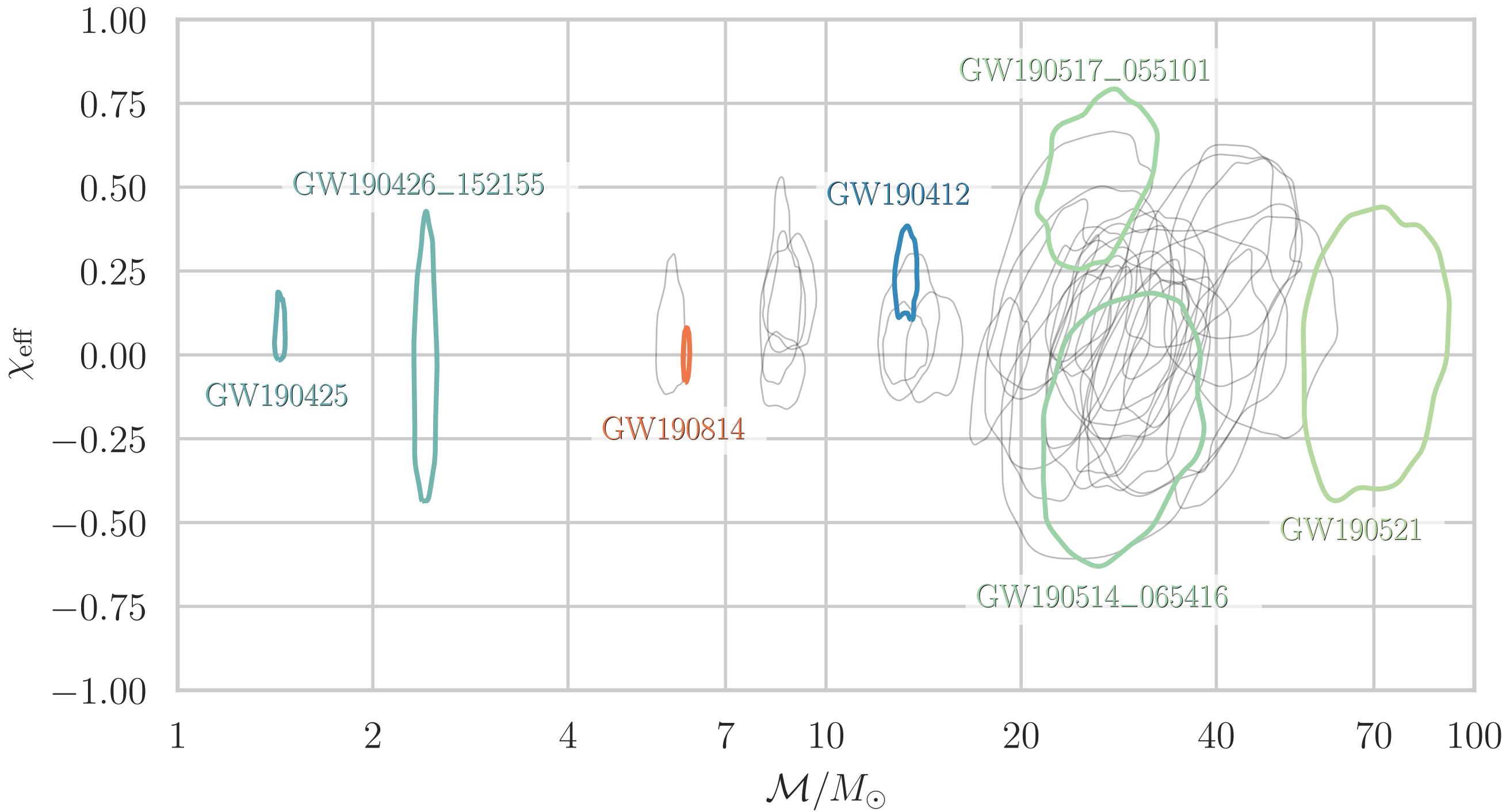
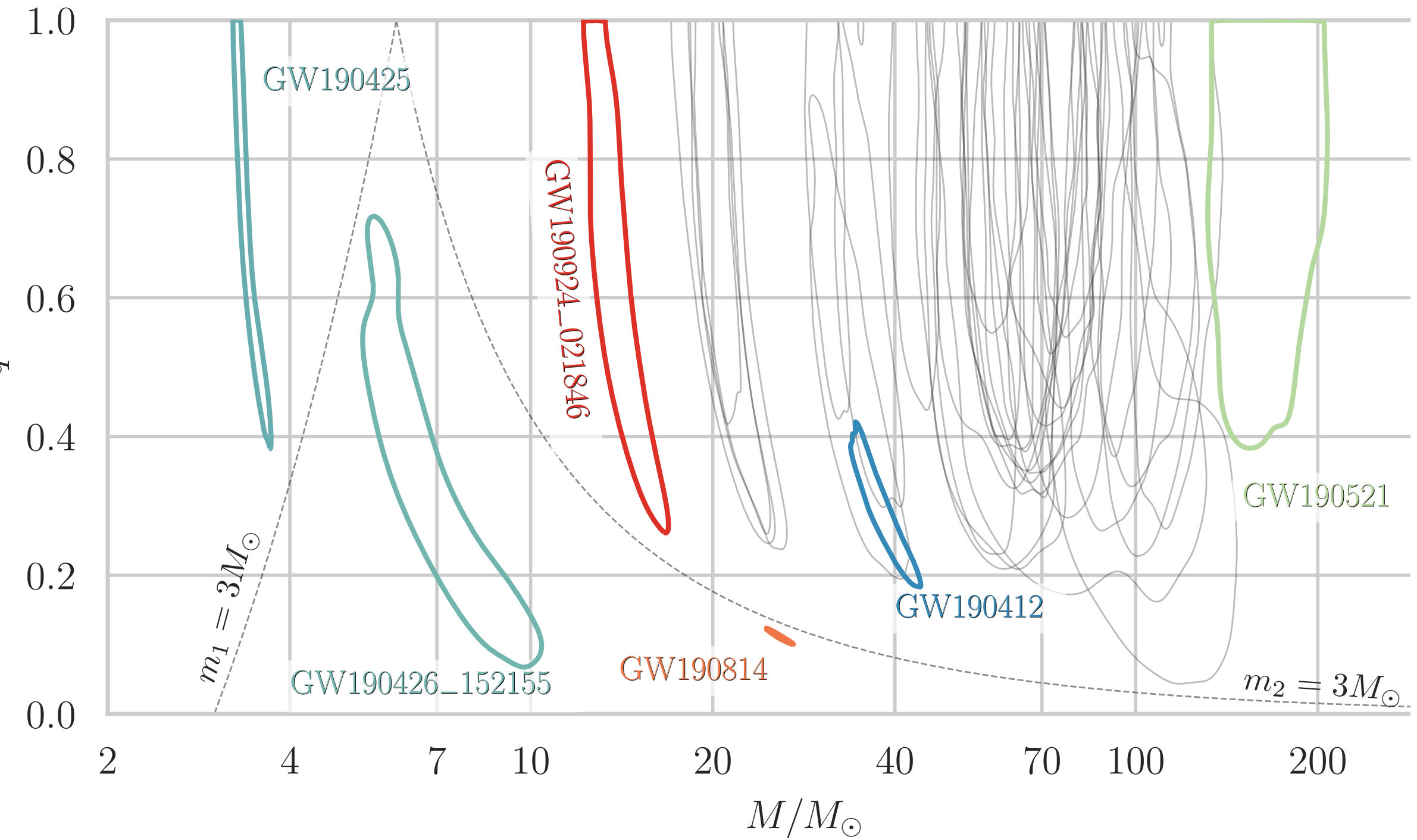
2
binary neutron star (BNS)



3-5
black hole - neutron star (BHNS)

The Gravitational-Wave Transient Catalogue (GWTC-2/3)

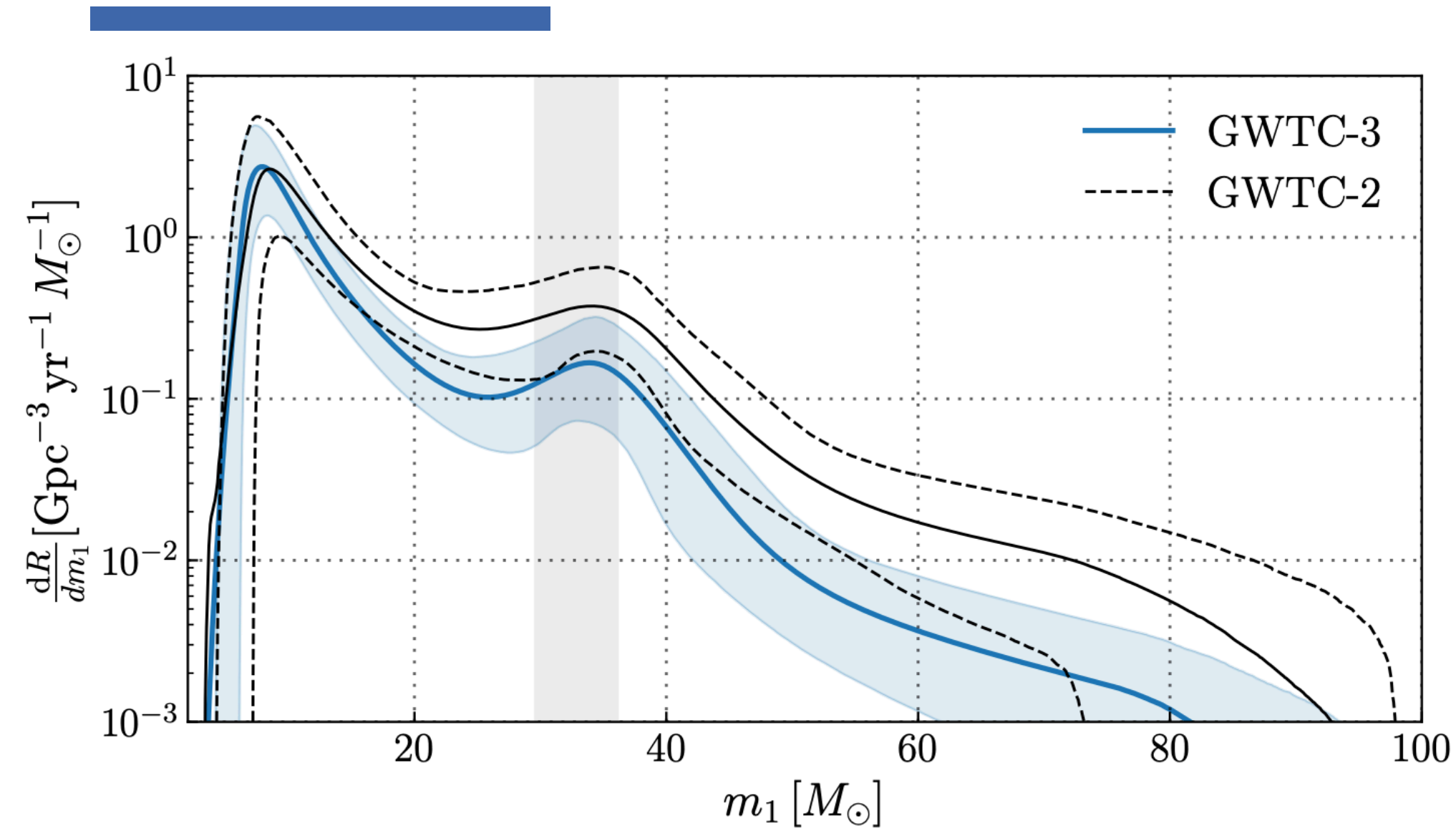
Abbot et al. arXiv:2010.14527 (2021)



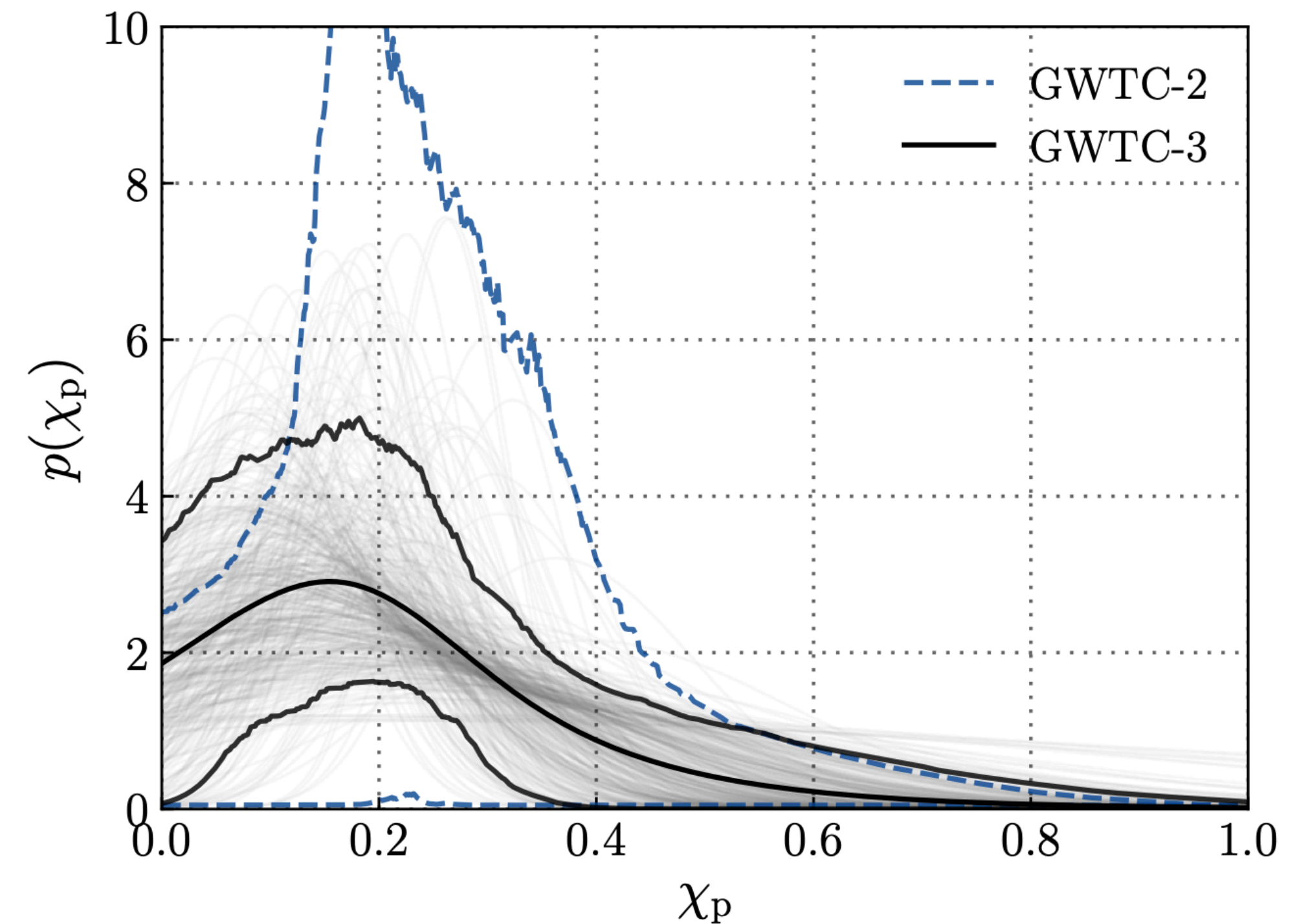
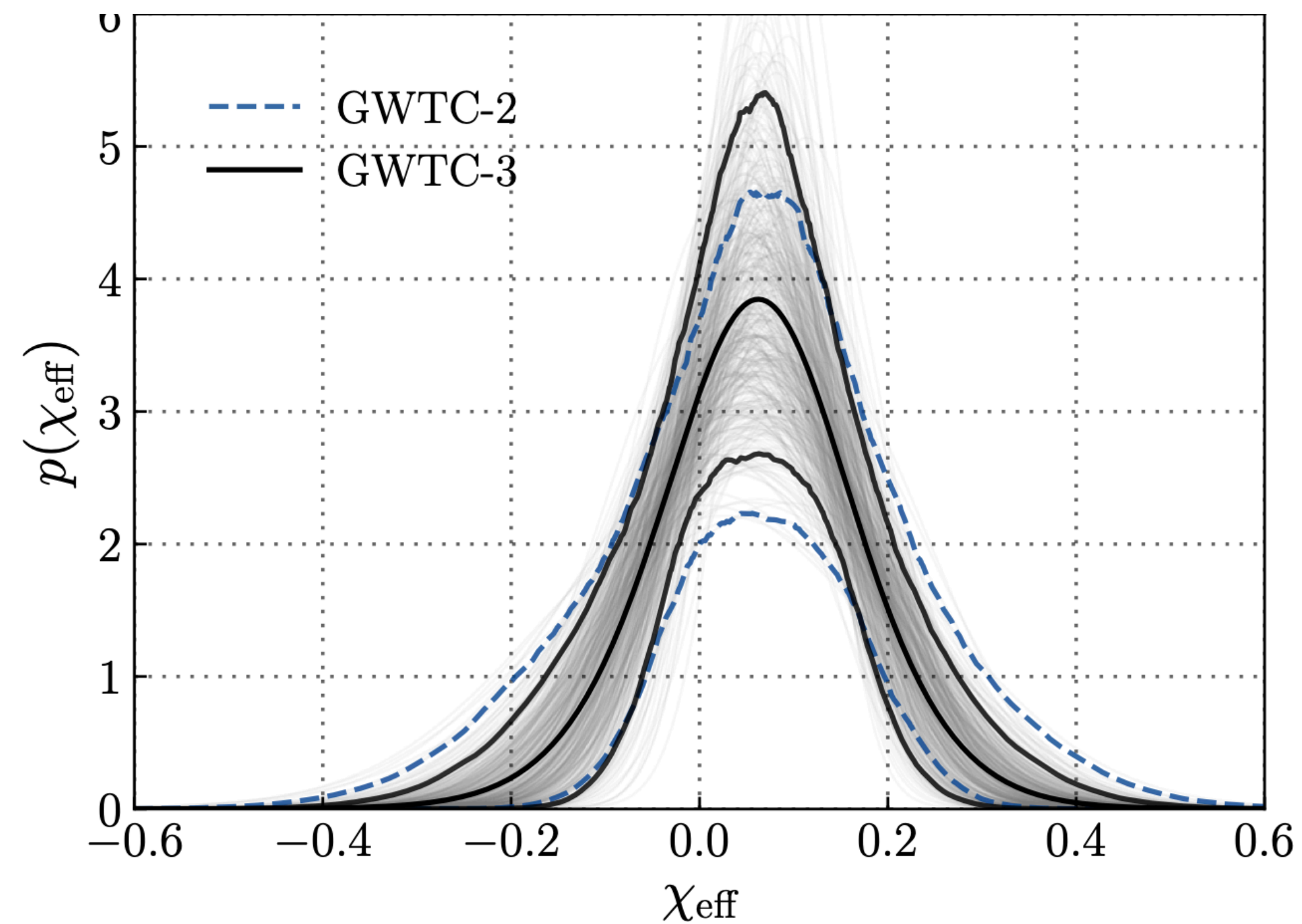
- **Heavy BHs,**
well into the “PISN mass-gap”
- **Light BHs,**
consistent with Galactic BH X-ray binaries
- **Unequal mass BBHs**
- **Heavy NSs,**
inconsistent with Galactic binary pulsars

- **Several BBHs with positive χ_{eff}**
(inconsistent with $\chi_{\text{eff}} = 0$)
- **No individual BBHs with negative χ_{eff}**
- **No individual BBHs inconsistent with $\chi_p = 0$**

Looking at coalescing BBH population properties



- **Several features emerge in the BH mass function**
- **Support for $\chi_{\text{eff}} \lesssim 0$ in the underlying BBH population**
- **Support for $\chi_p > 0$ in the underlying BBH population**
- **Caution: conclusions are model-dependent!**



Correlation of gravitational-wave observables

Chirp mass: $M_{\text{chirp}} = \frac{(m_1 m_2)^{3/5}}{(m_1 + m_2)^{1/5}}$

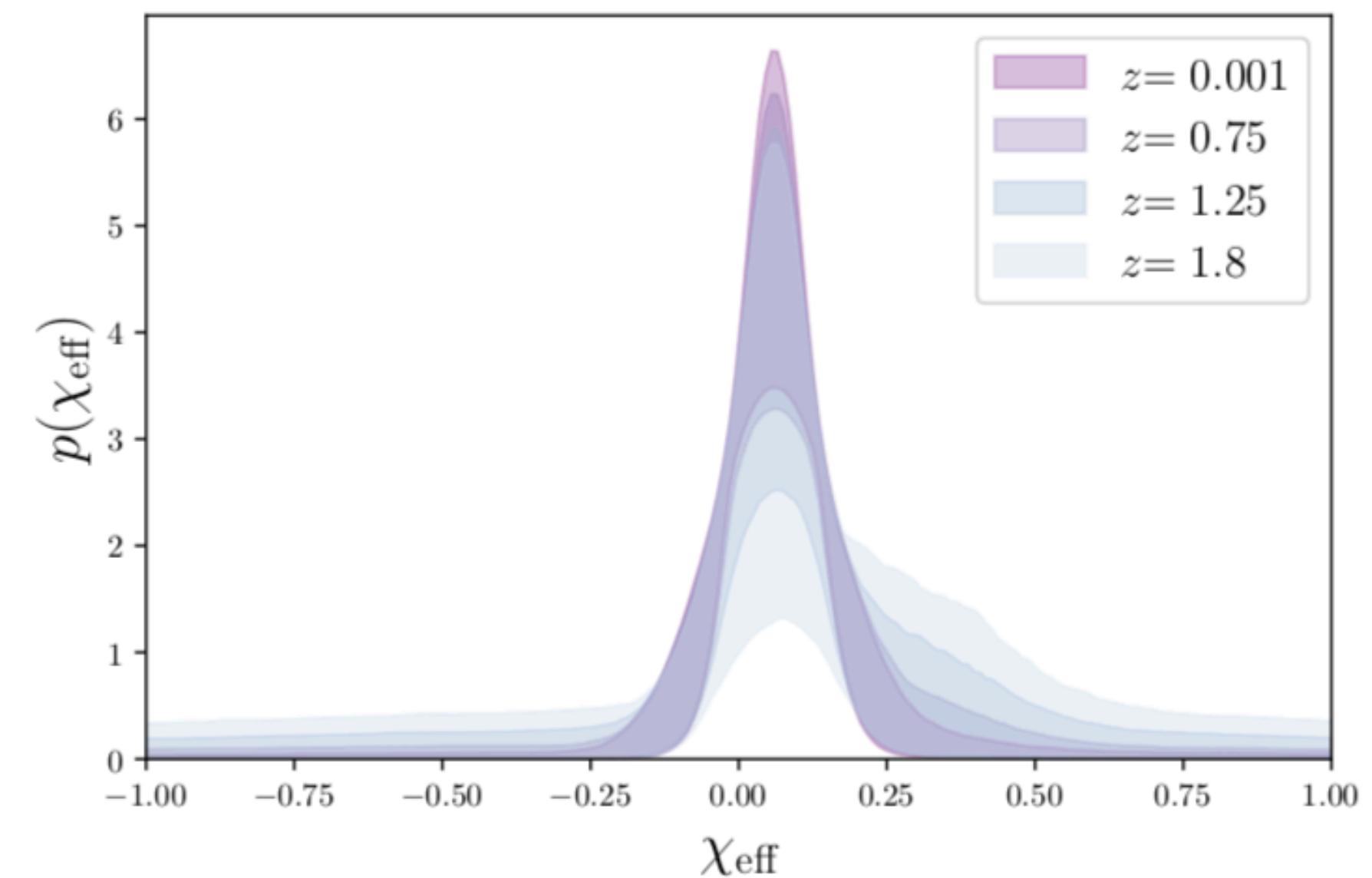
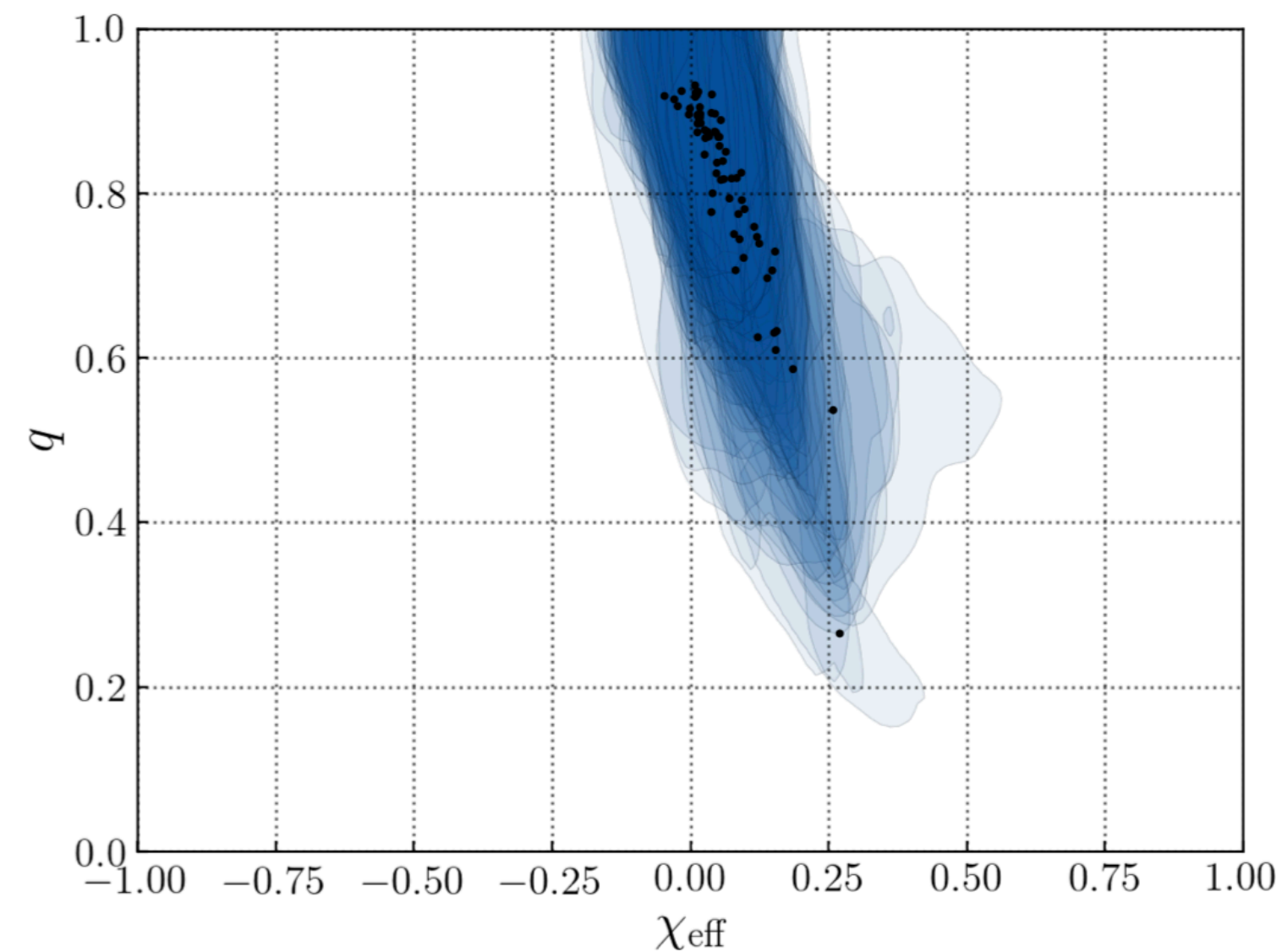
Effective spin parameter: $\chi_{\text{eff}} = \frac{m_1 \vec{\chi}_1 + m_2 \vec{\chi}_2}{m_1 + m_2} \cdot \hat{L}$

Merger redshift: z_{merger}

Mass ratio: q

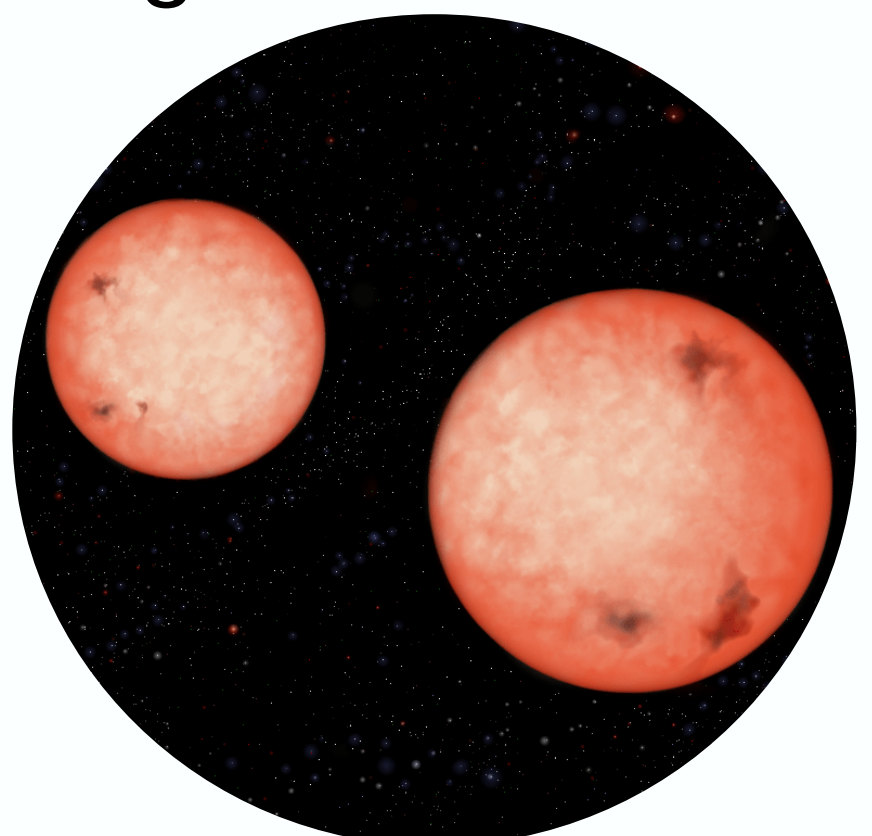
Indications appear already in the O3 LVC data, e.g.,

- Correlation between M_{chirp} and χ_{eff}
e.g. Franciolini & Pain (2022), Safarzadeh et al. (2020)
- Anti-correlation between χ_{eff} and mass ratio q
e.g., Callister et al. (2021), Abbott et al. (2021)
- Correlation between χ_{eff} and merger redshift z
e.g., Biscoveanu et al. (2022), Bavera, ..., TF et al. (2022)



Astrophysical binary black-hole formation models

Isolated binary evolution in galactic fields



e.g. Sigurdsson & Hernquist (1993), Zwart & McMillan (2000), Miller & Lauburg (2009), Rodriguez et al. (2015), Antonini et al. (2016), Mapelli (2016), Askar et al. (2017)

Common Envelope:
e.g. vd Heuvel (1976), Tutukov & Yungelson (1993), Kalogera et al. (2007), Postnov & Yungelson (2014), Belczynski et al. (2016), Mapelli et al. (2017)

Stable Mass Transfer:
e.g. van den Heuvel et al. (2017), Pavlovskii et al. (2017), Inayoshi et al. (2017)

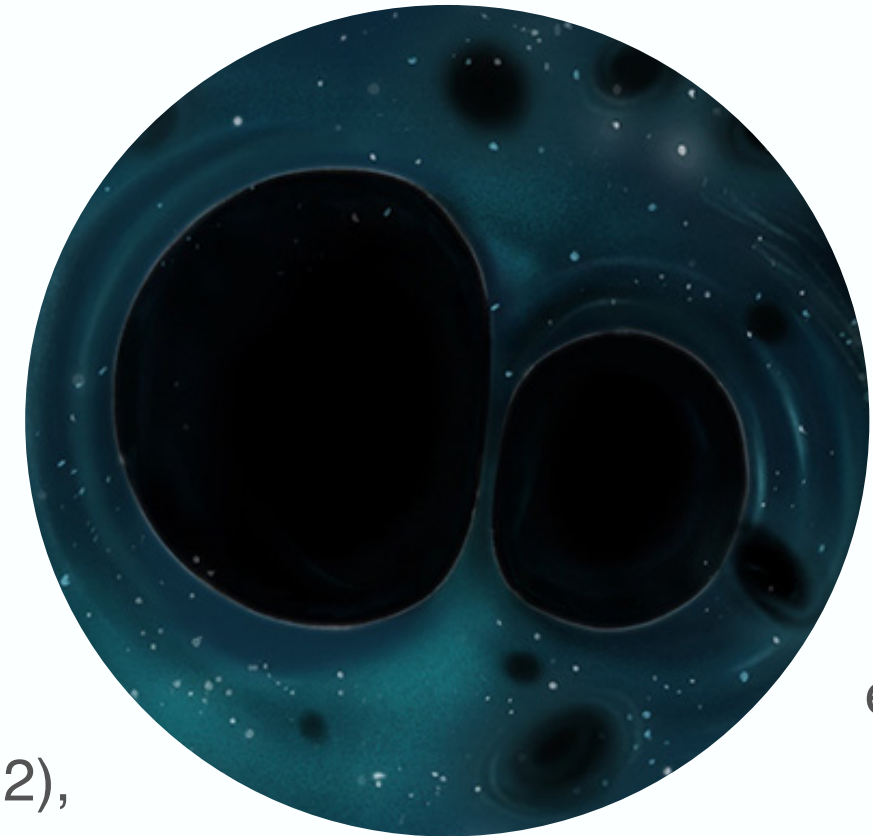
Chemically homogeneous evolution:
e.g. Maeder (1987), de Mink et al. (2009), Mandel & de Mink (2016), Marchant et al. (2016)

Population III stars



e.g. Inayoshi et al. (2017)

Primordial black holes



e.g. Antonini & Perets (2012), Tagawa et al. (2020)

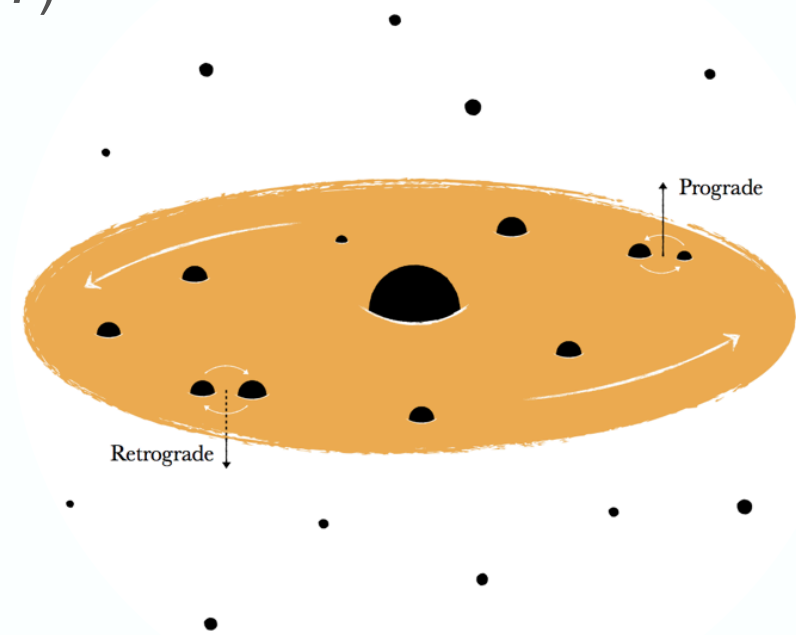
e.g., Bird et al. (2016); Sasaki et al. (2018); Clesse & Garcia-Bellido (2020); Da Luca et al. (2020,2021) Wong et al. (2021)

& MORE ...

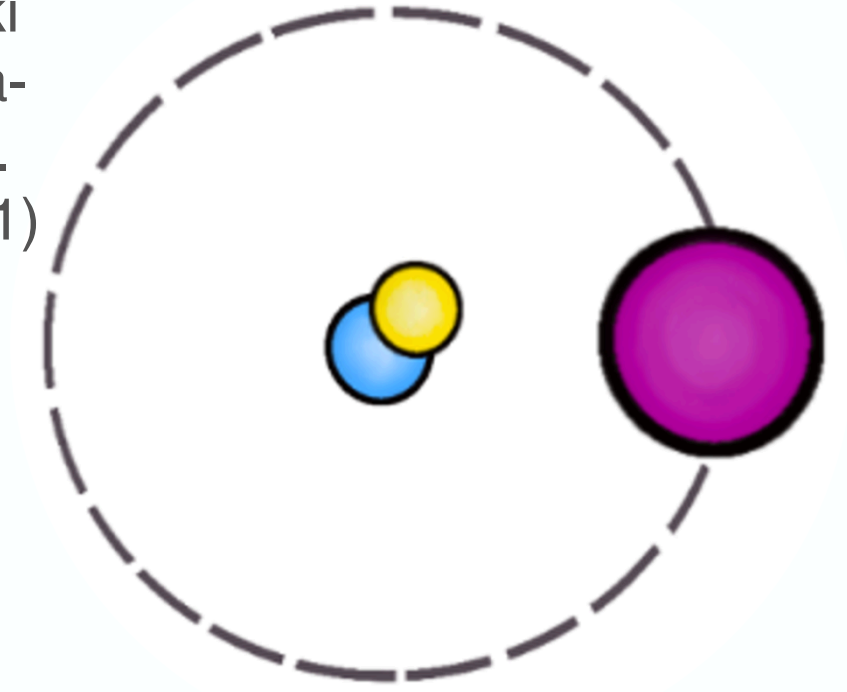
e.g. Silsbee & Tremaine (2017), Moe & Di Stefano (2017); Toonen et al. (2022)



Dynamical formation in dense stellar environments



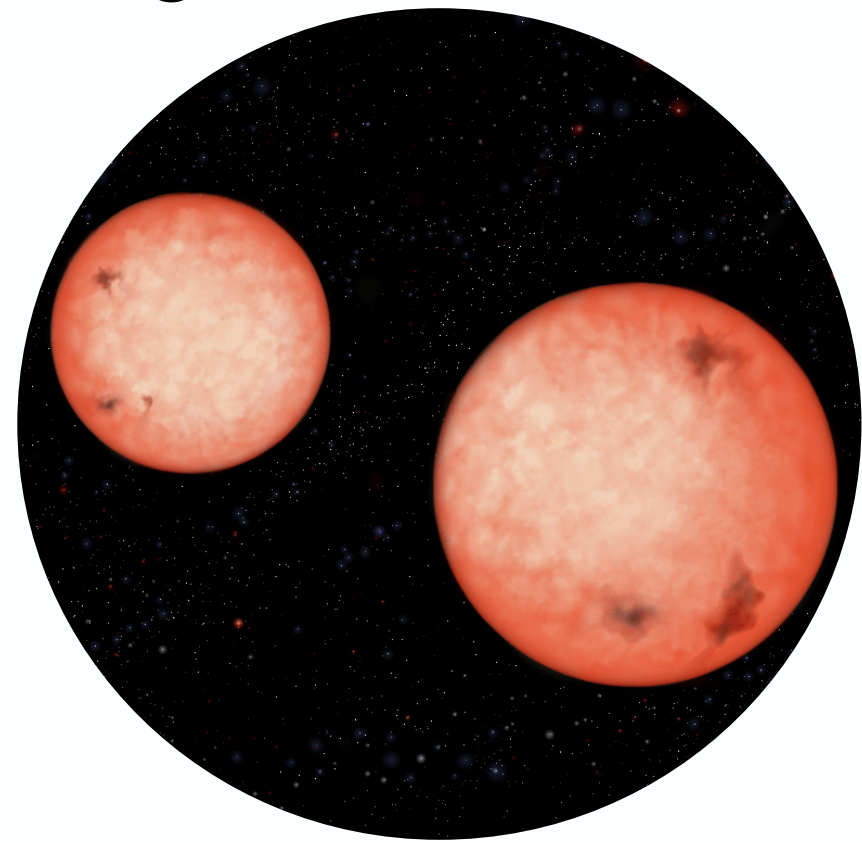
Active galactic nuclei disks



Triple and multiples

Binary black-hole formation channels

Isolated binary evolution in galactic fields



e.g. Sigurdsson & Hernquist (1993), Zwart & McMillan (2000), Miller & Lauburg (2009), Rodriguez et al. (2015), Antonini et al. (2016), Mapelli et al. (2017), Askar et al. (2017)

Common Envelope:

e.g. vd Heuvel (1976), Tutukov & Yungelson (1993), Kalogera et al. (2007), Postnov & Yungelson (2014), Belczynski et al. (2016), Mapelli et al. (2017)

Stable Mass Transfer:

e.g. van den Heuvel et al. (2017), Paczynski et al. (2017), Inayoshi et al. (2017)

Chemically homogeneous evolution:

e.g. Maeder (1987), de Mink et al. (2009), Mandel & de Mink (2016), Marchant et al. (2016)

Dynamical formation in dense stellar environments

Population III stars

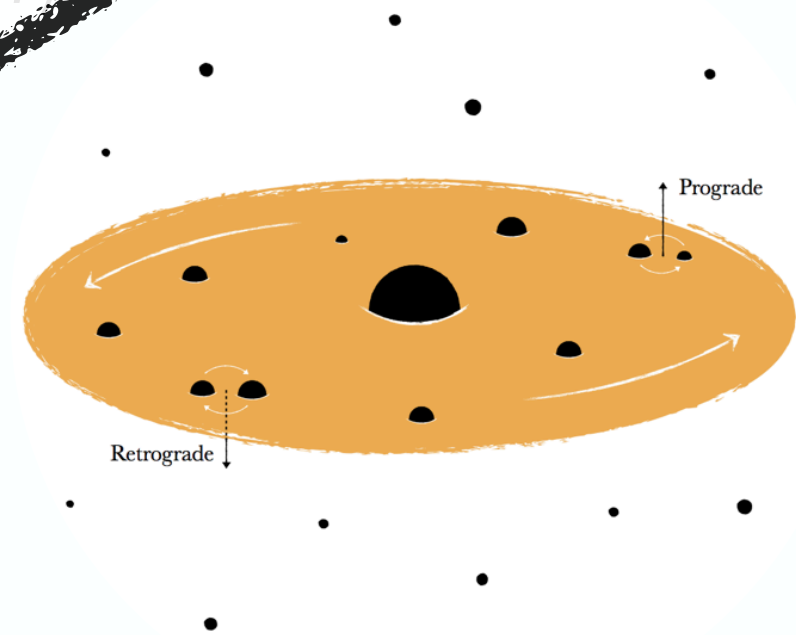


Primordial black holes



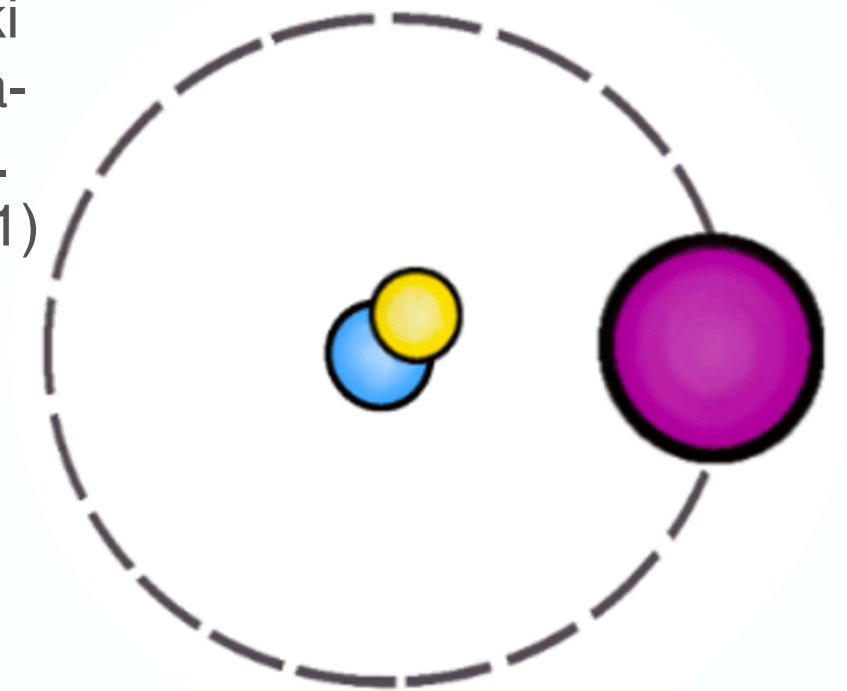
& MORE ...

Rates cannot distinguish among the channels
e.g. see Mandel & Broekgaarden (2022)



Active galactic nuclei disks

e.g., Bird et al. (2016); Sasaki et al. (2018); Clesse & Garcia-Bellido (2020); Da Luca et al. (2020,2021) Wong et al. (2021)



Triple and multiples

What can cause a black-hole to spin?

Angular momentum of the progenitor star

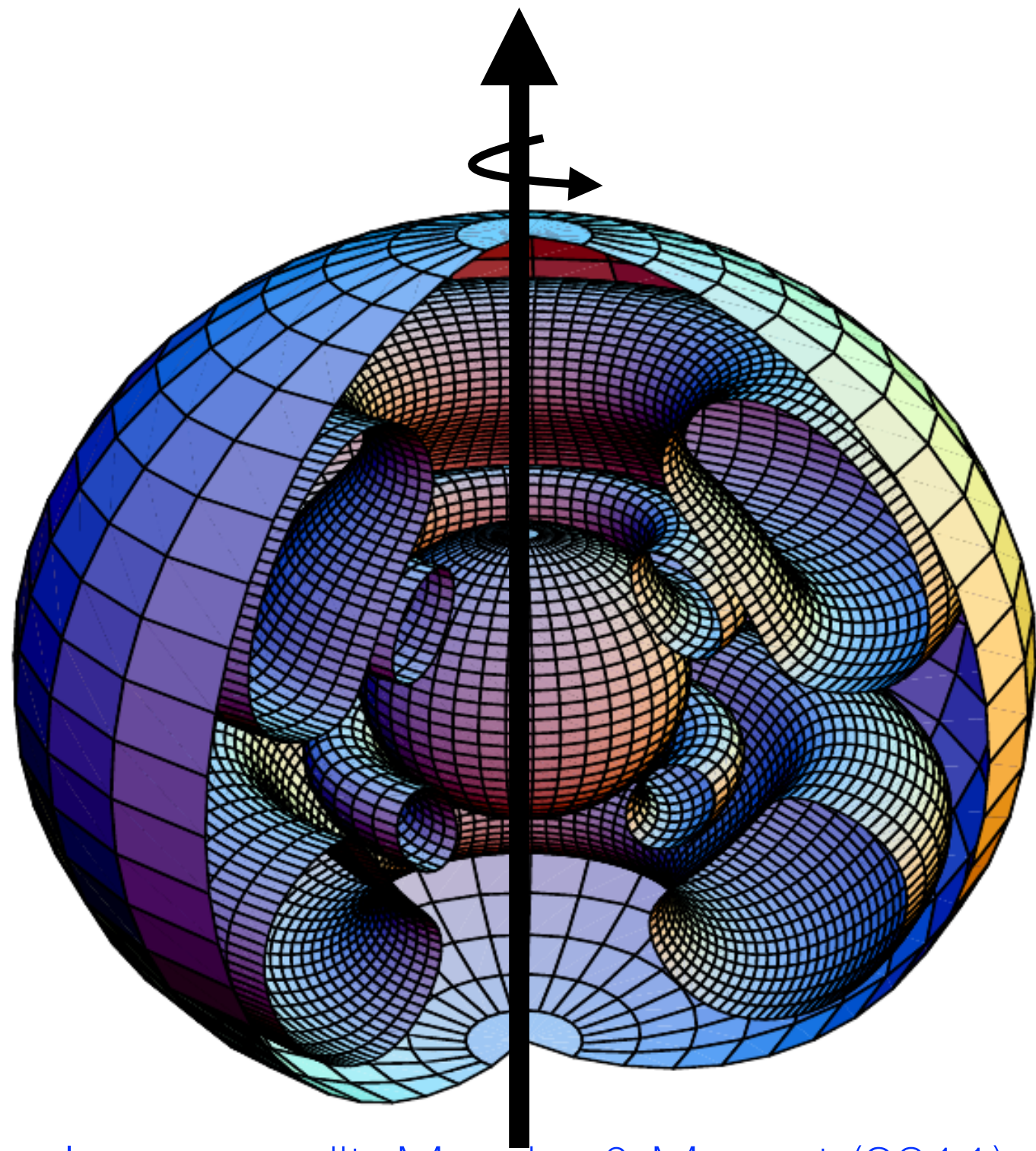


Image credit: Maeder & Meynet (2011)

Unknown process during core-collapse

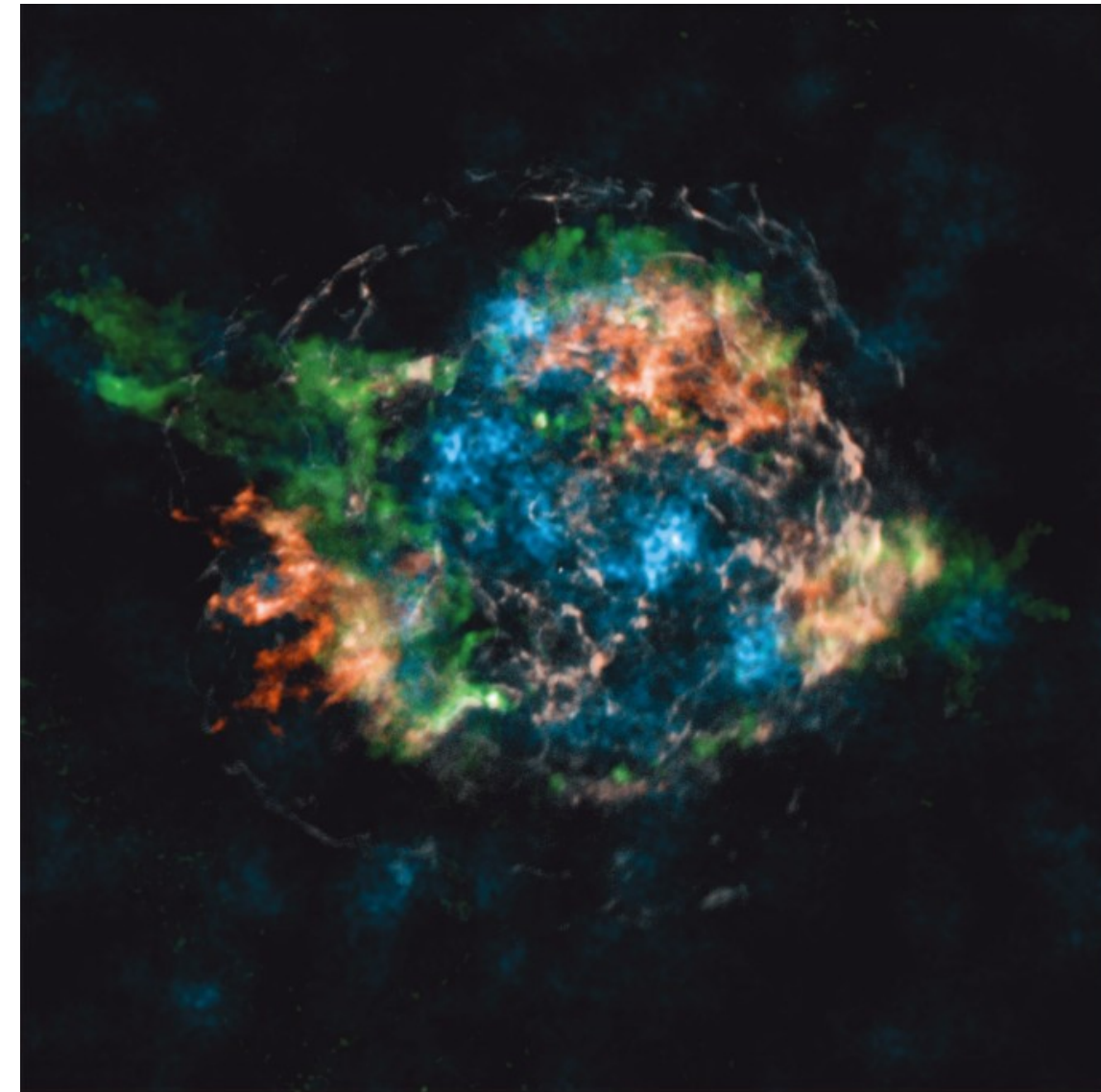


Image credit: Grefenstette et al. (2014)

Accretion onto a black hole

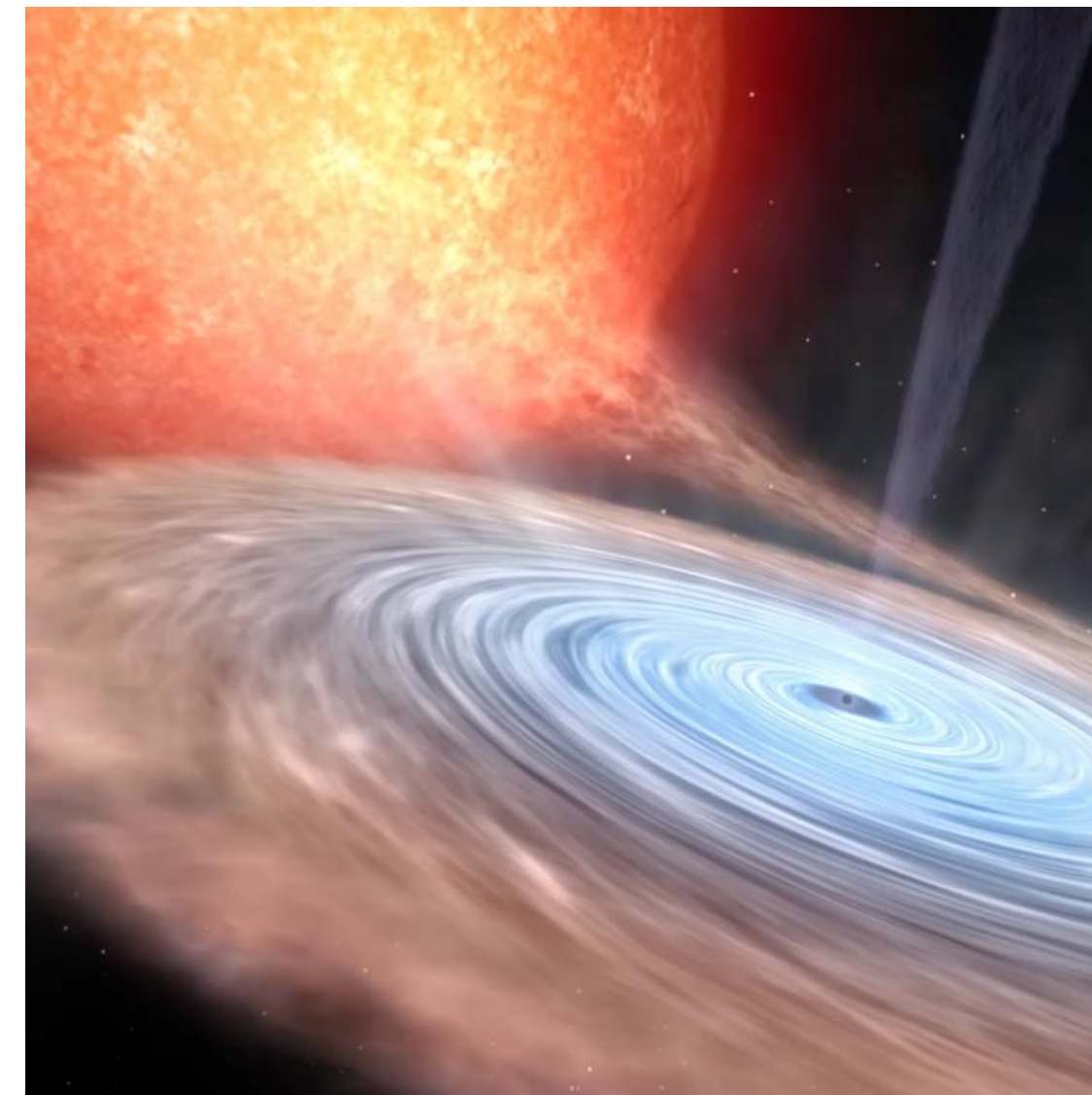


Image credit: Gabriel Pérez

Hierarchical mergers

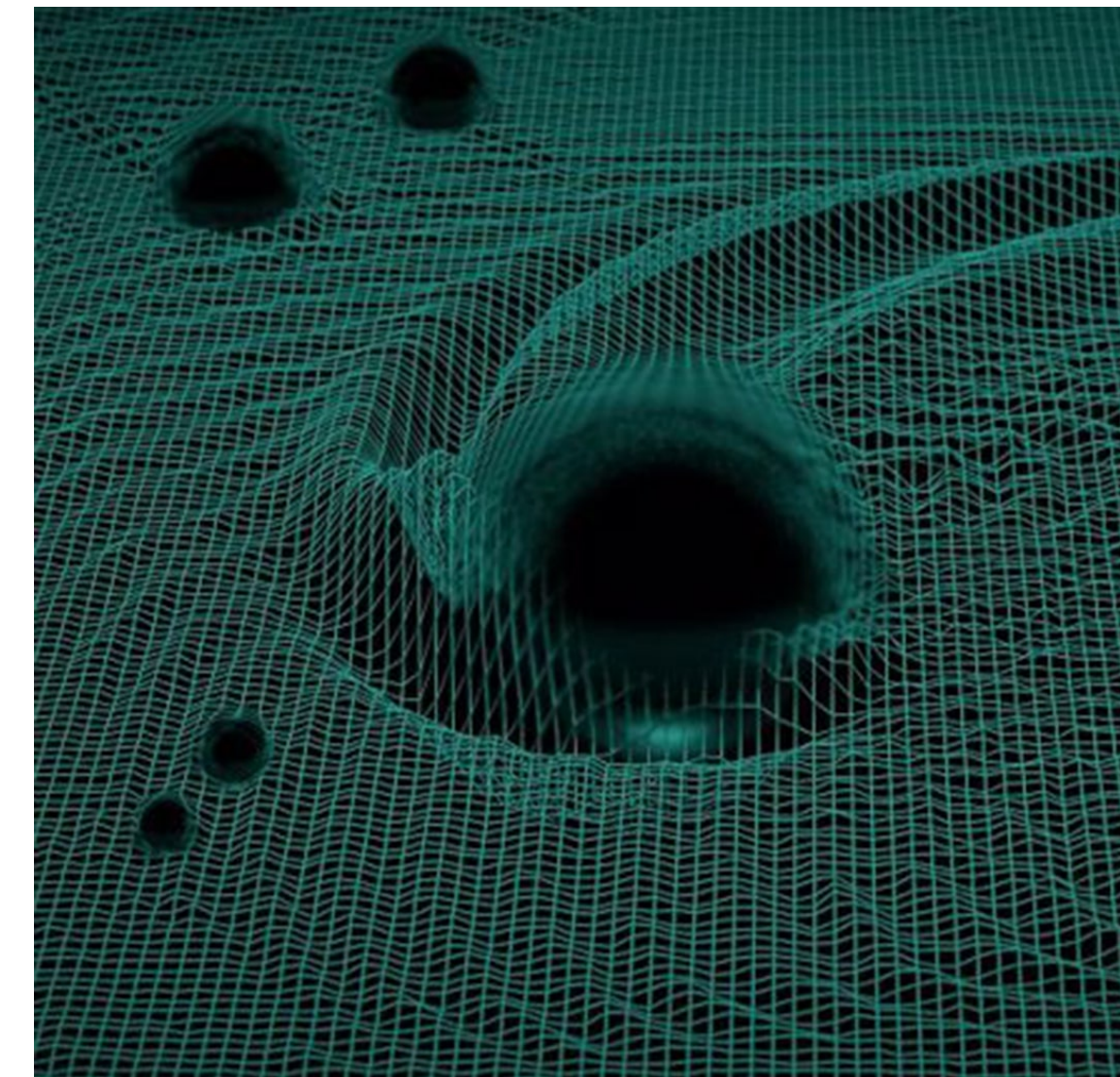


Image credit: Riccardo Buscichio

What can cause a black-hole to spin?

See e.g.,
Moreno-Mendez & Cantiello 2016
Fuller et al. 2015

Angular momentum
of the progenitor star

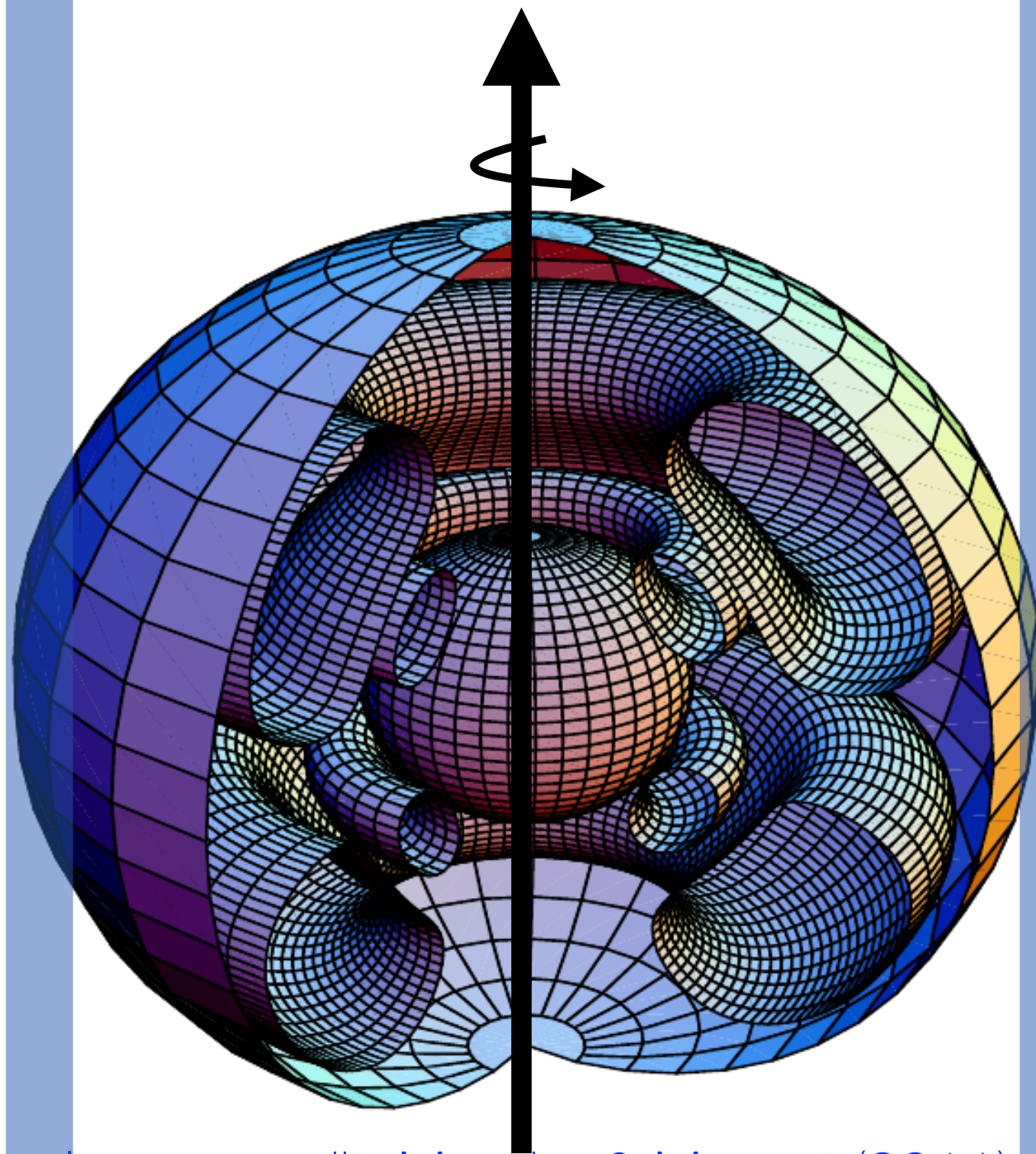


Image credit: Maeder & Meynet (2011)

Unknown process
during core-collapse

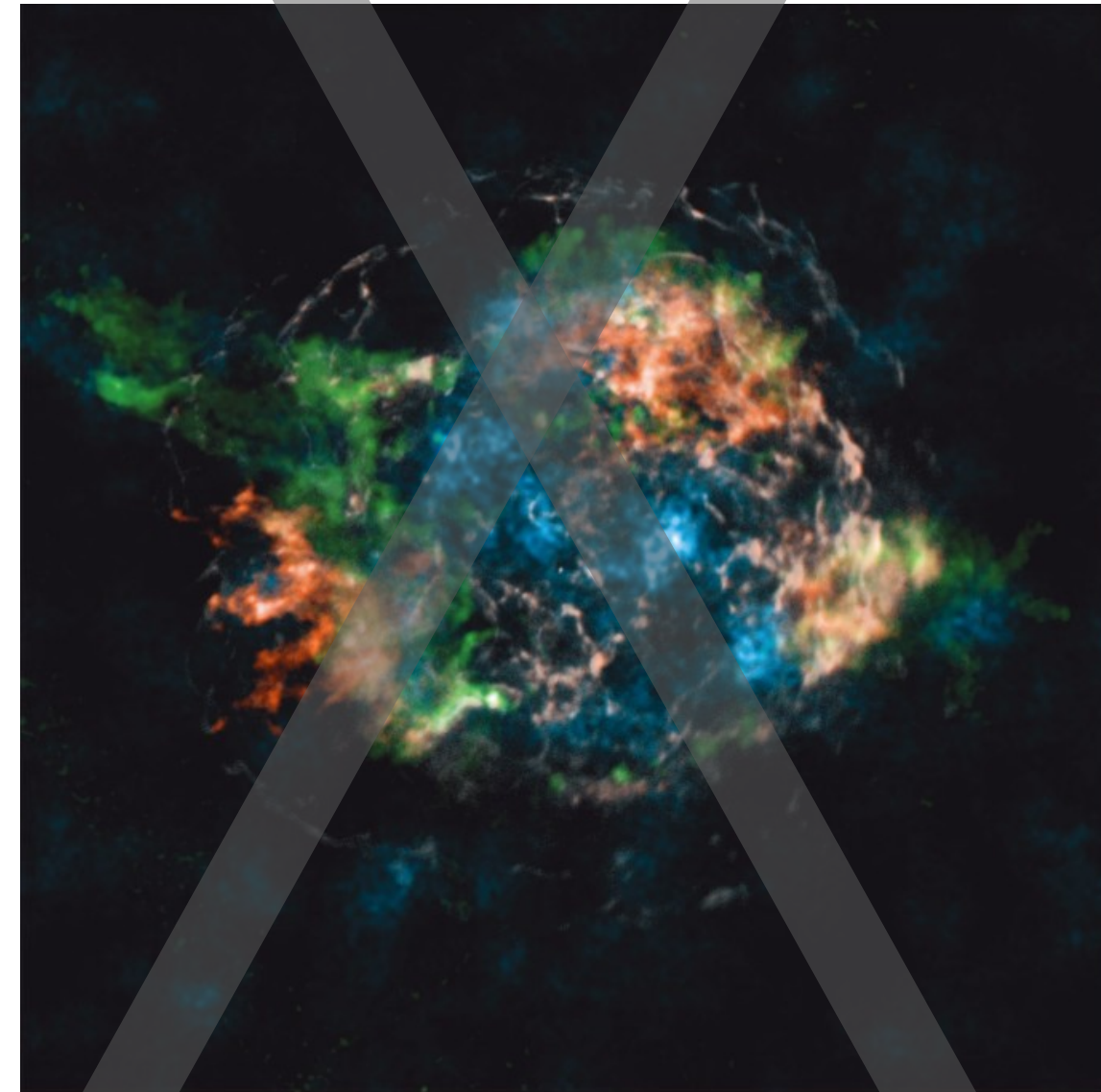


Image credit: Grefenstette et al. (2014)

Accretion onto a
black hole

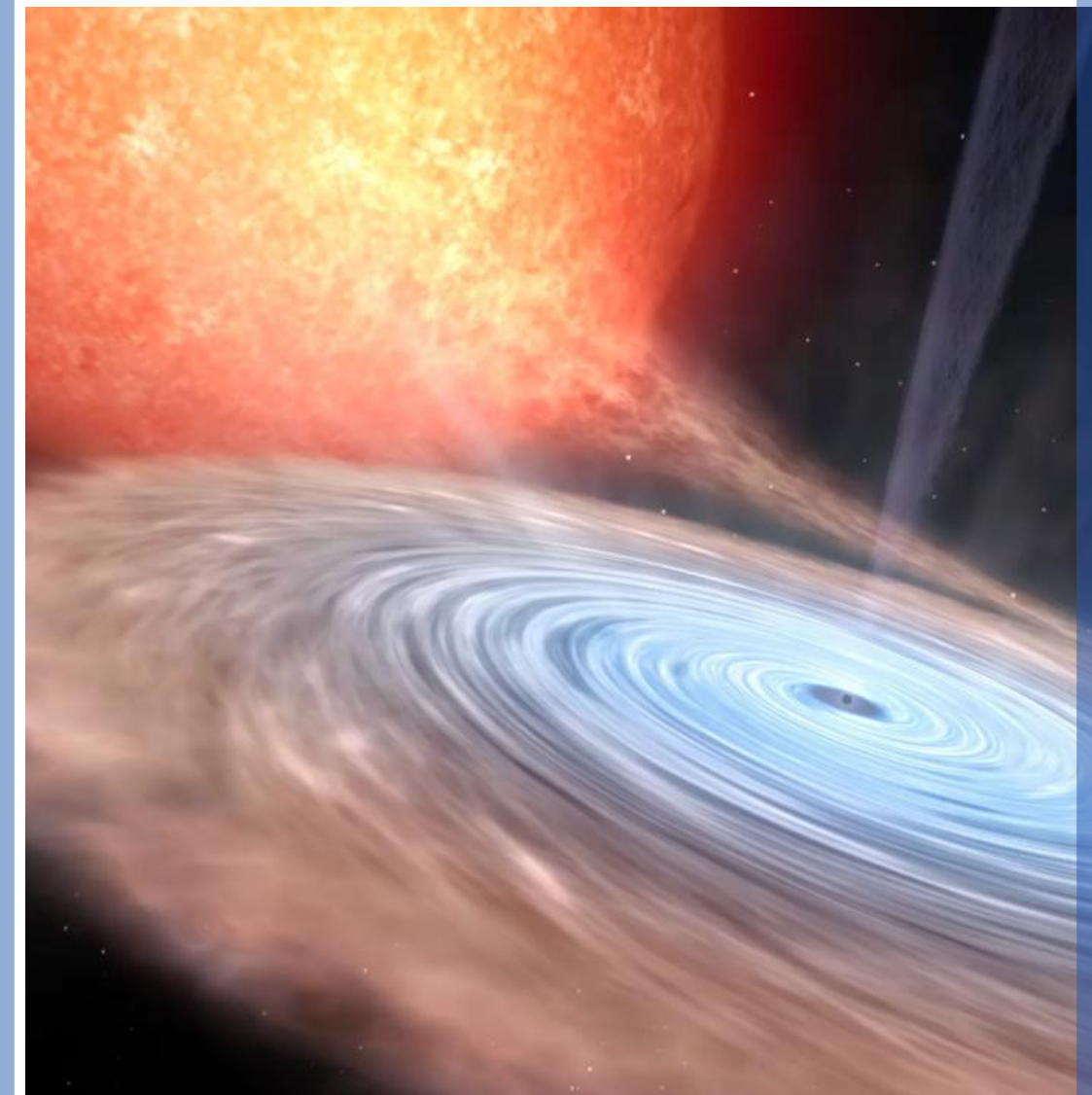


Image credit: Gabriel Pérez

Hierarchical
mergers

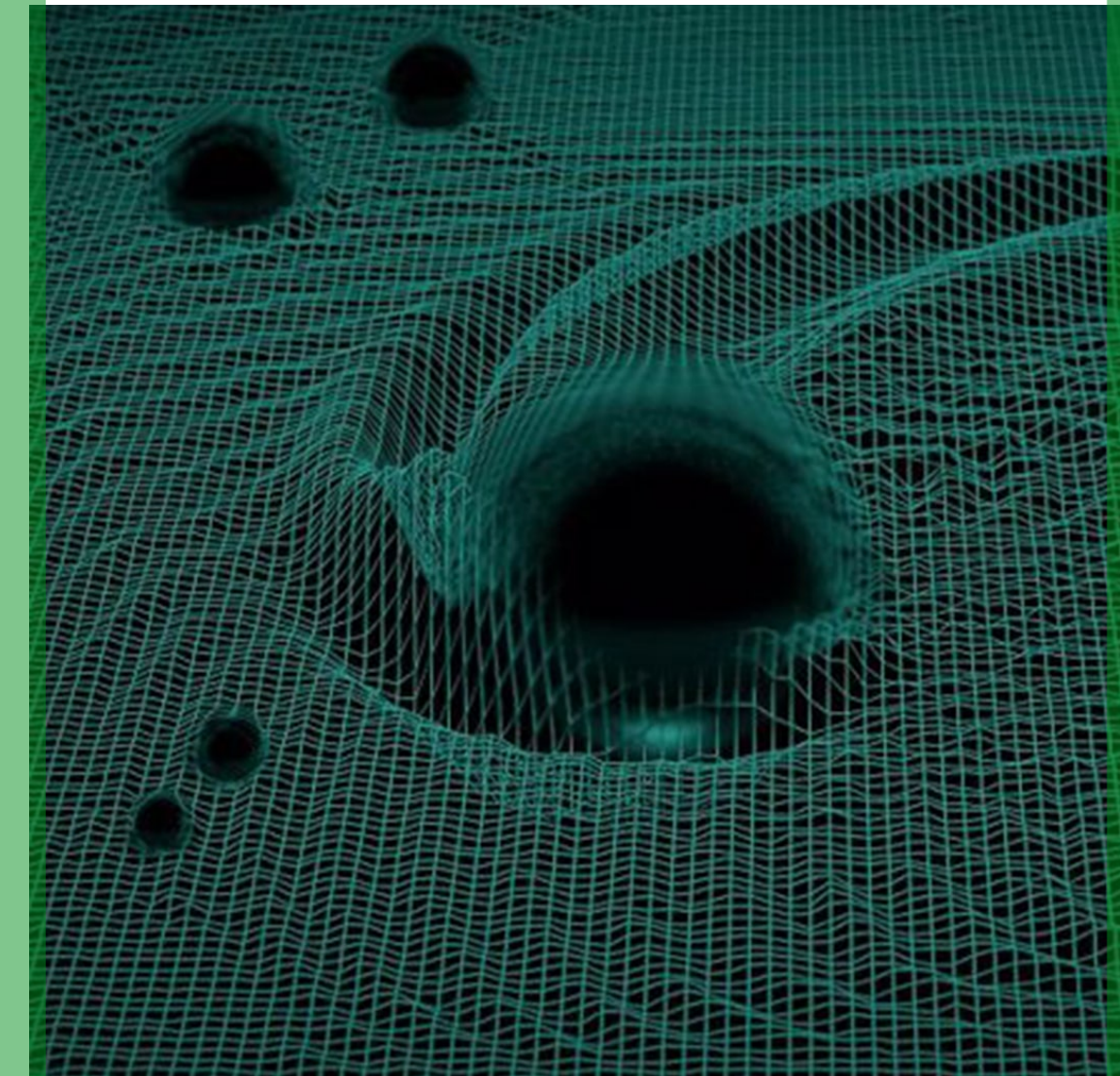
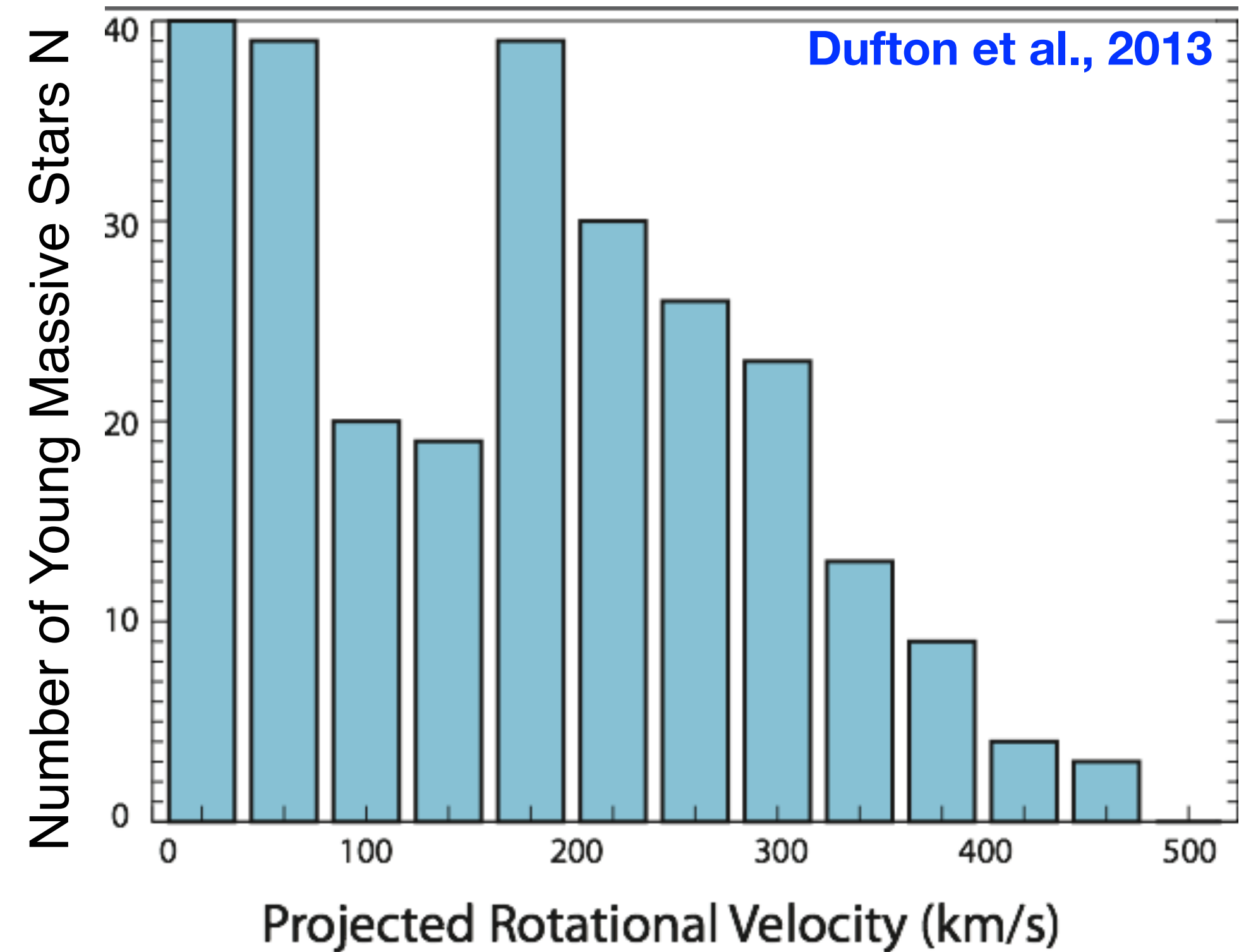
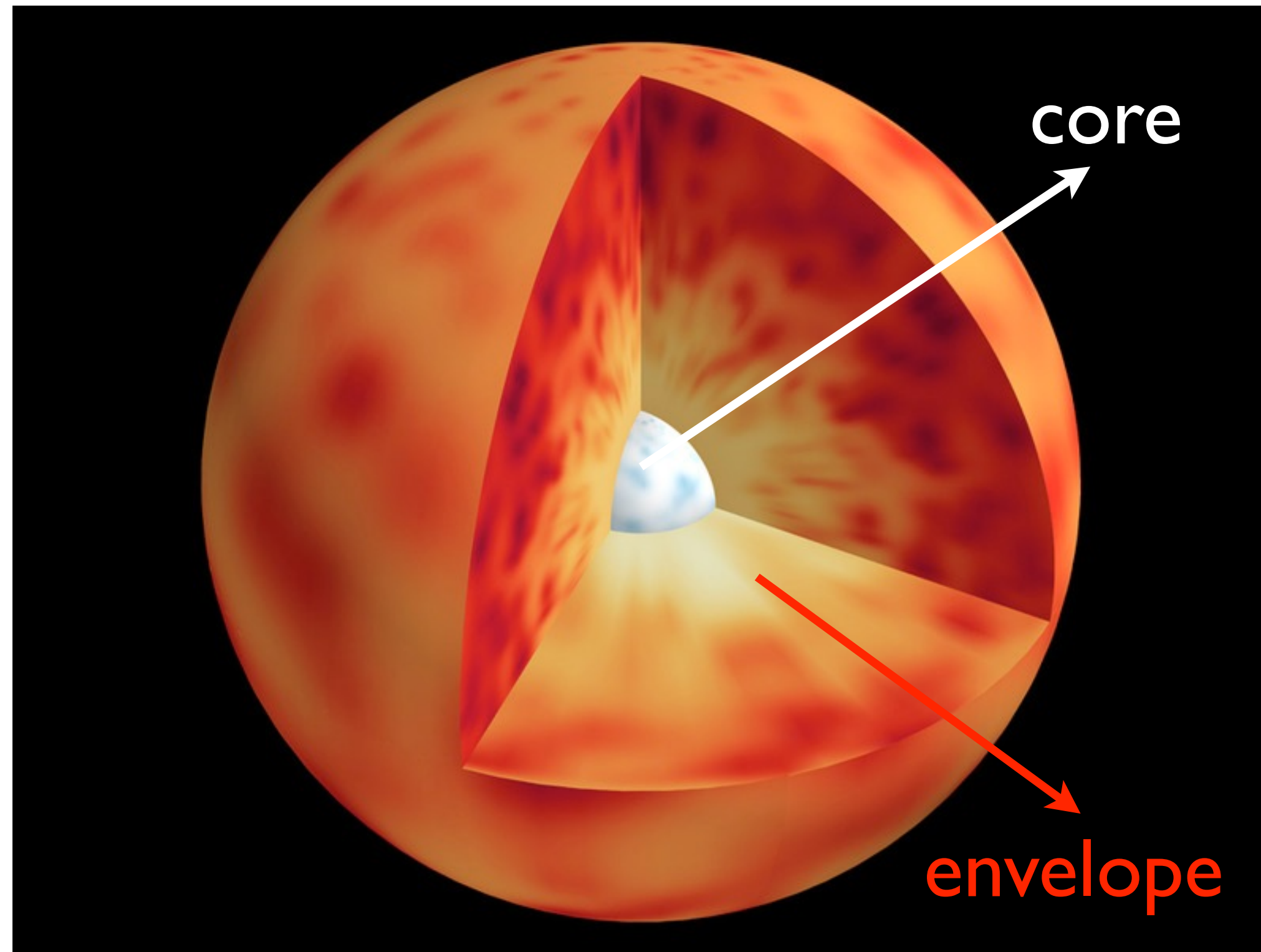


Image credit: Riccardo Buscichio

Stellar rotation

The question of the origin of black hole spin is inherently related to the rotation of massive stars.

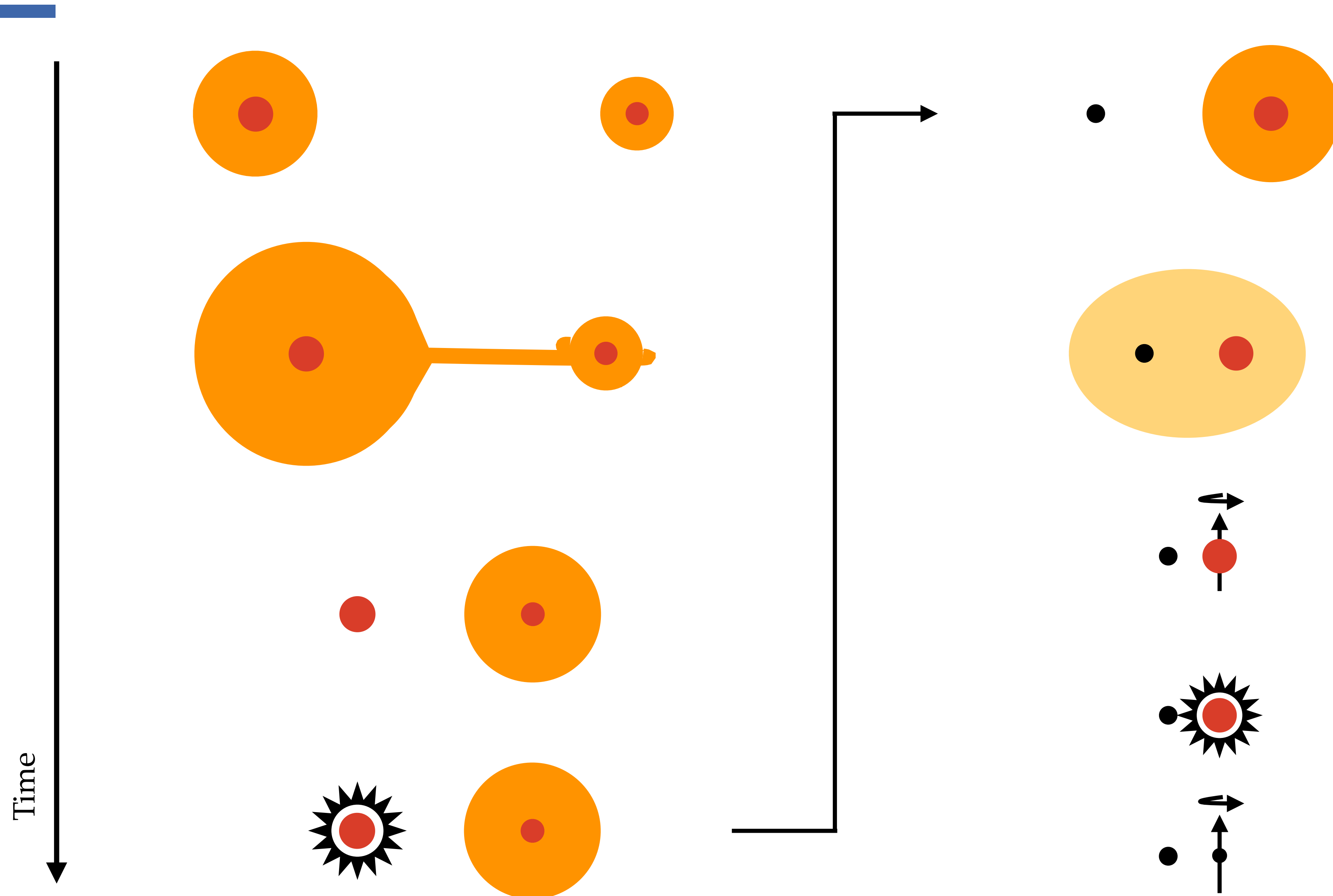


Constraints from asteroseismic observations of low mass (sub-)giants and rotation rates of young neutron stars and white dwarves point towards efficient **angular momentum transport**.

e.g. Kurtz et al. 2014; Deheuvels et al. 2015; Gehan et al. 2018, Langer et al. 2012, Fuller et al. 2019

The common envelope formation scenario

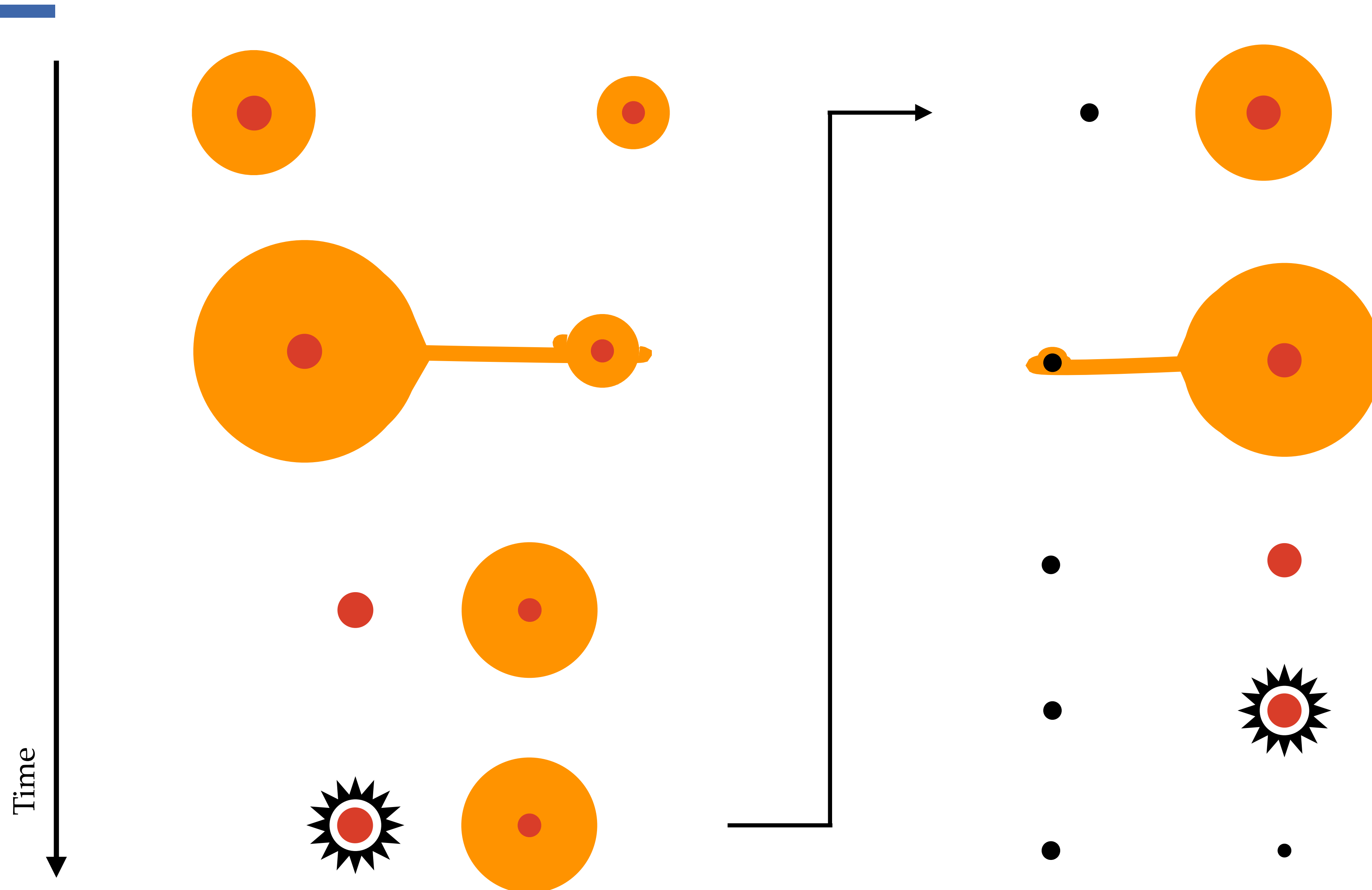
$P_{ZAMS} \sim 100$ days



e.g., van den Heuvel (1976), Kalogera et al. (2007), Dominik et al. (2012, 2013, 2015), Belczynski et al. (2016, 2020), Bavera et al. (2020, 2021a, 2022a,c)

The stable mass transfer formation scenario

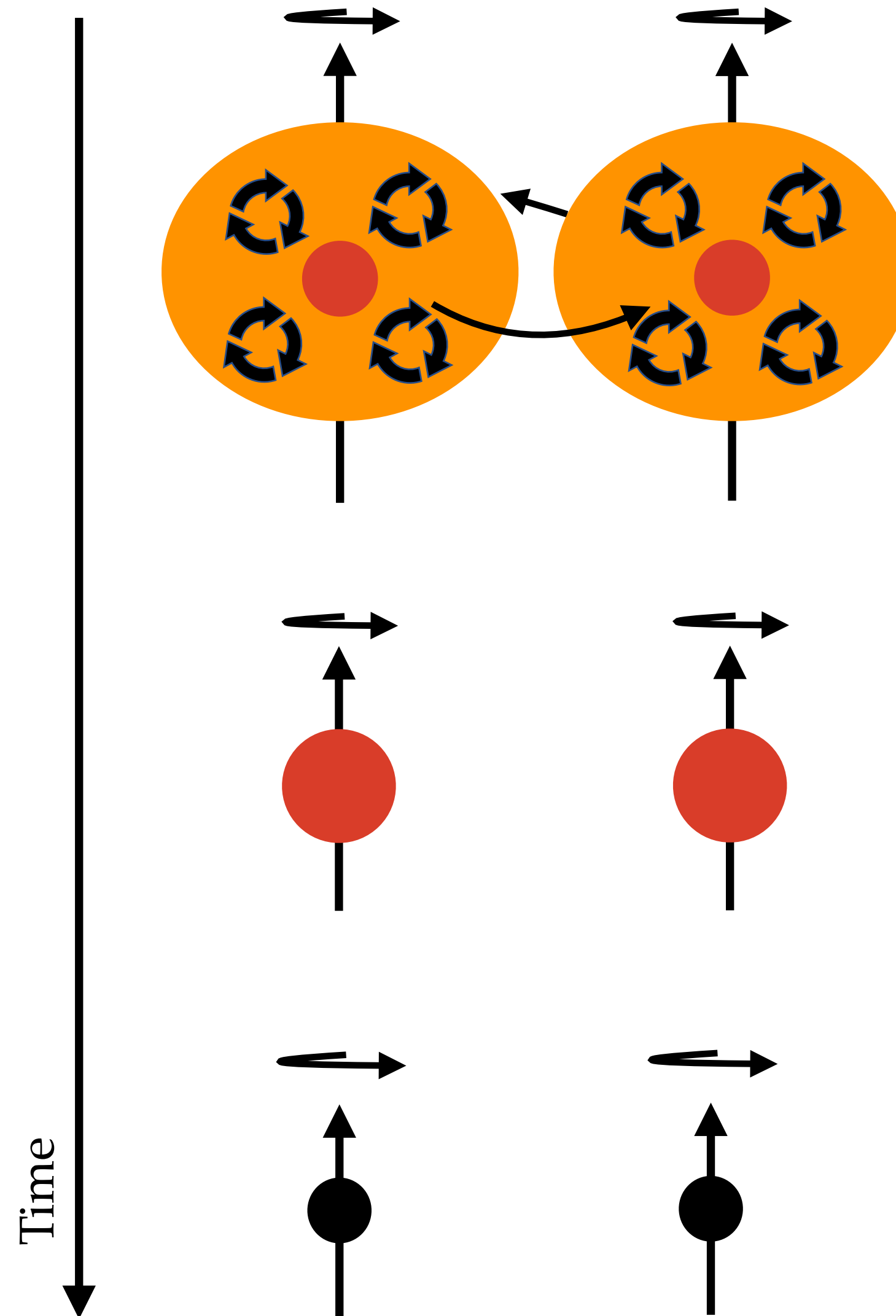
$p_{\text{ZAMS}} \sim 10$ days



e.g., Pavlovskii et al. (2017), van den Heuvel et al. (2017), Neijssel et al. (2019), van Son et al. (2021), Bavera et al. (2021a, 2022a,c)

The chemically homogeneous evolution scenario

$$P_{\text{ZAMS}} \lesssim 1 \text{ day}$$



e.g., Marchant et al. (2016), de Mink & Mandel (2016), du Buisson et al. (2021), Riley et al. (2021), Bavera et al. (2022a,c)

Binary population synthesis



Initial binary
population
(ZAMS)

~10M binaries

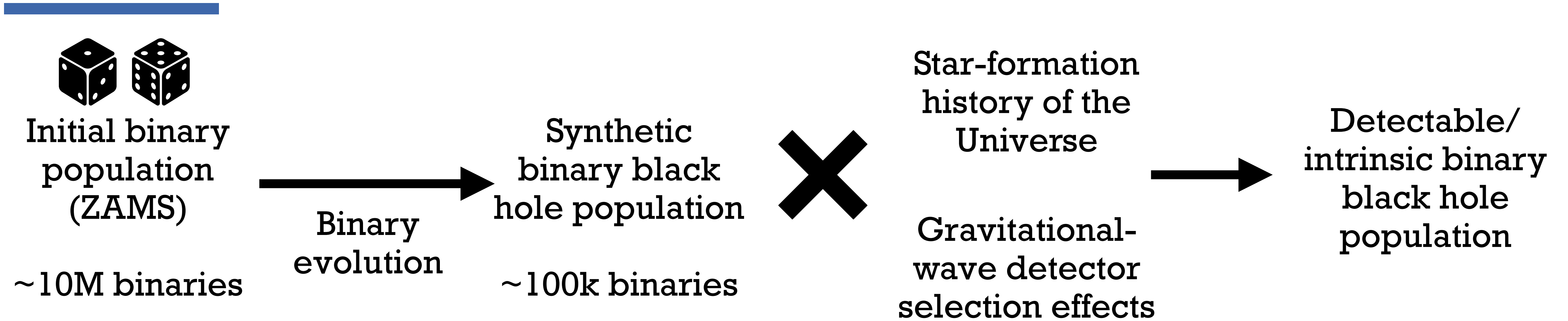


Binary
evolution

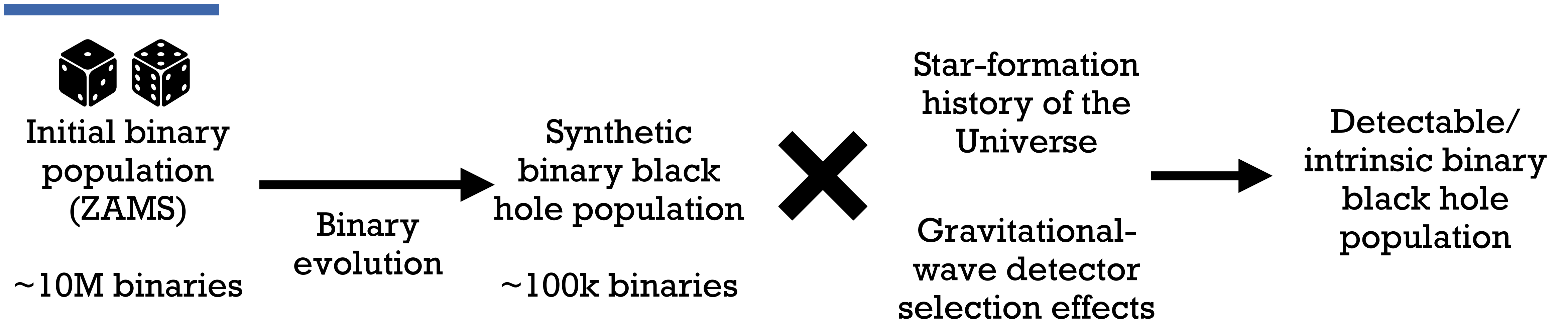
Synthetic
binary black
hole population

~100k binaries

Binary population synthesis



Binary population synthesis



Binary evolution simulation tools:

- Rapid (parametric) binary evolution:

PRO: fast ~1 CPU second.

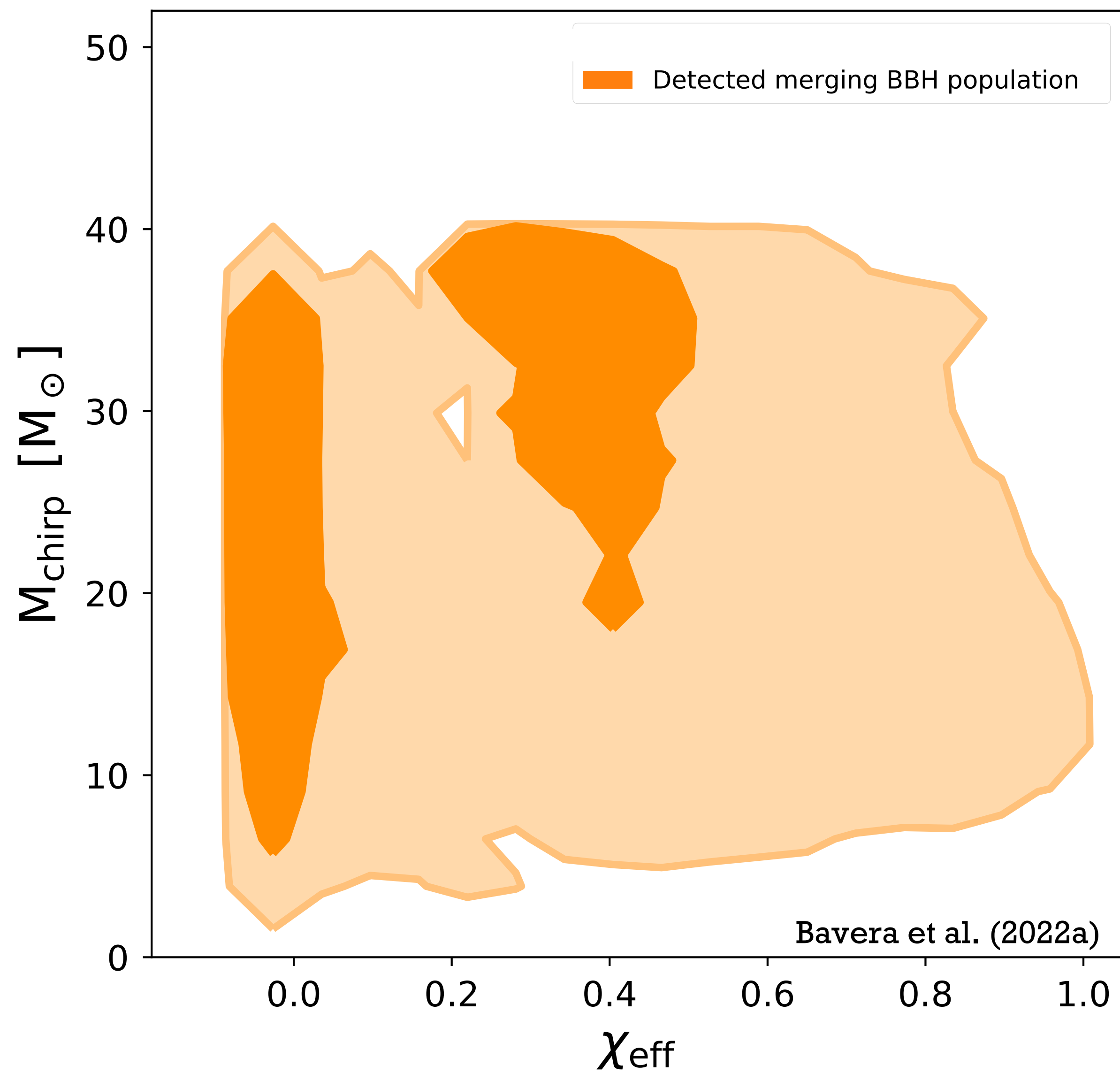
CON: approximate star's evolution and binary interactions with fitting formulae.

- Detailed binary evolution:

PRO: accurate modelling of binary interactions and feedbacks on stellar evolution.

CON: slow ~ 10-100 CPU hours.

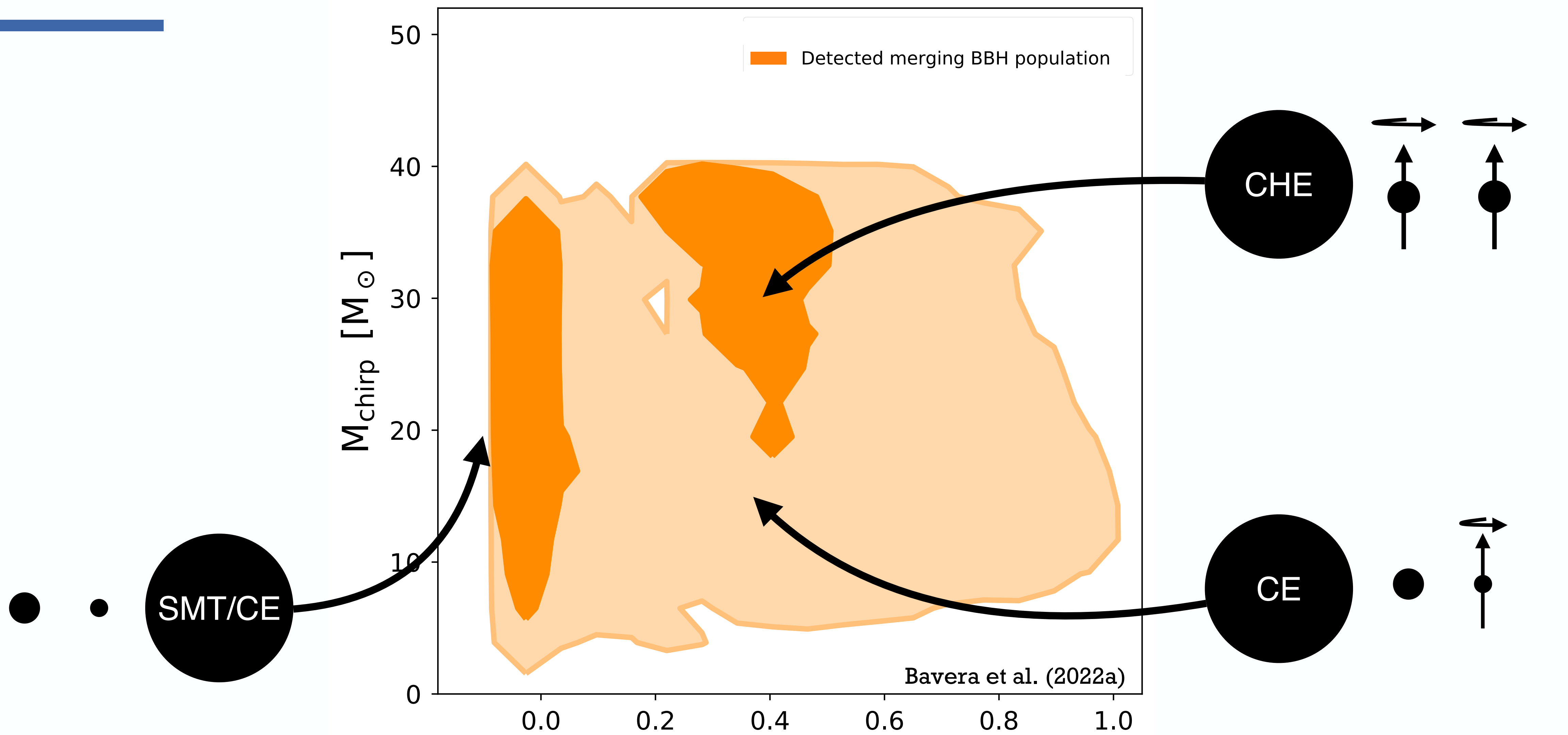
Binary black hole mass-spin distribution



Chirp mass: $M_{\text{chirp}} = \frac{(m_1 m_2)^{3/5}}{(m_1 + m_2)^{1/5}}$

Effective spin parameter: $\chi_{\text{eff}} = \frac{m_1 \vec{\chi}_1 + m_2 \vec{\chi}_2 \cdot \hat{L}}{m_1 + m_2}$

Binary black hole mass-spin distribution

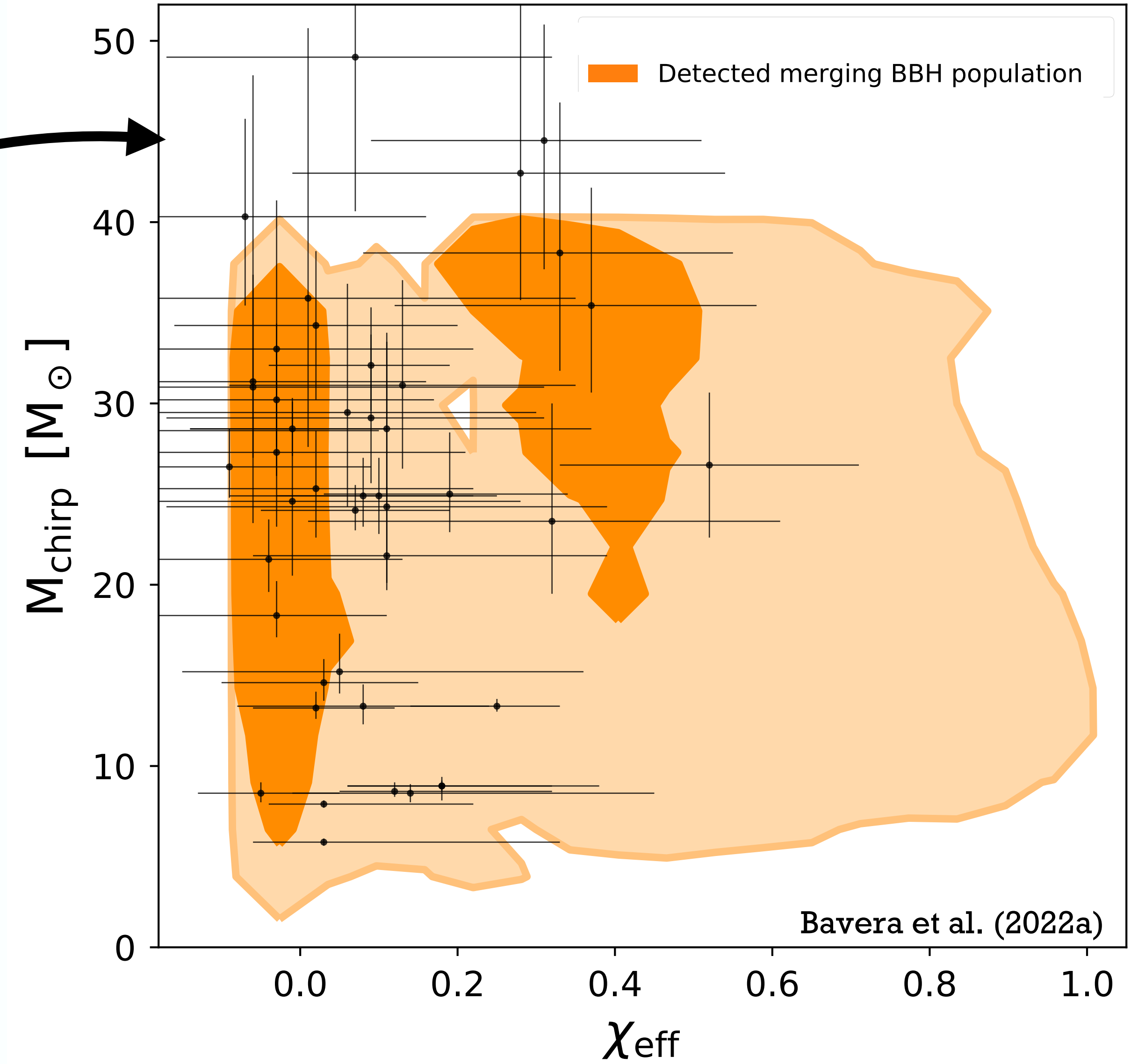


Chirp mass: $M_{\text{chirp}} = \frac{(m_1 m_2)^{3/5}}{(m_1 + m_2)^{1/5}}$

Effective spin parameter: $\chi_{\text{eff}} = \frac{m_1 \vec{\chi}_1 + m_2 \vec{\chi}_2 \cdot \hat{L}}{m_1 + m_2}$

Binary black hole mass-spin distribution

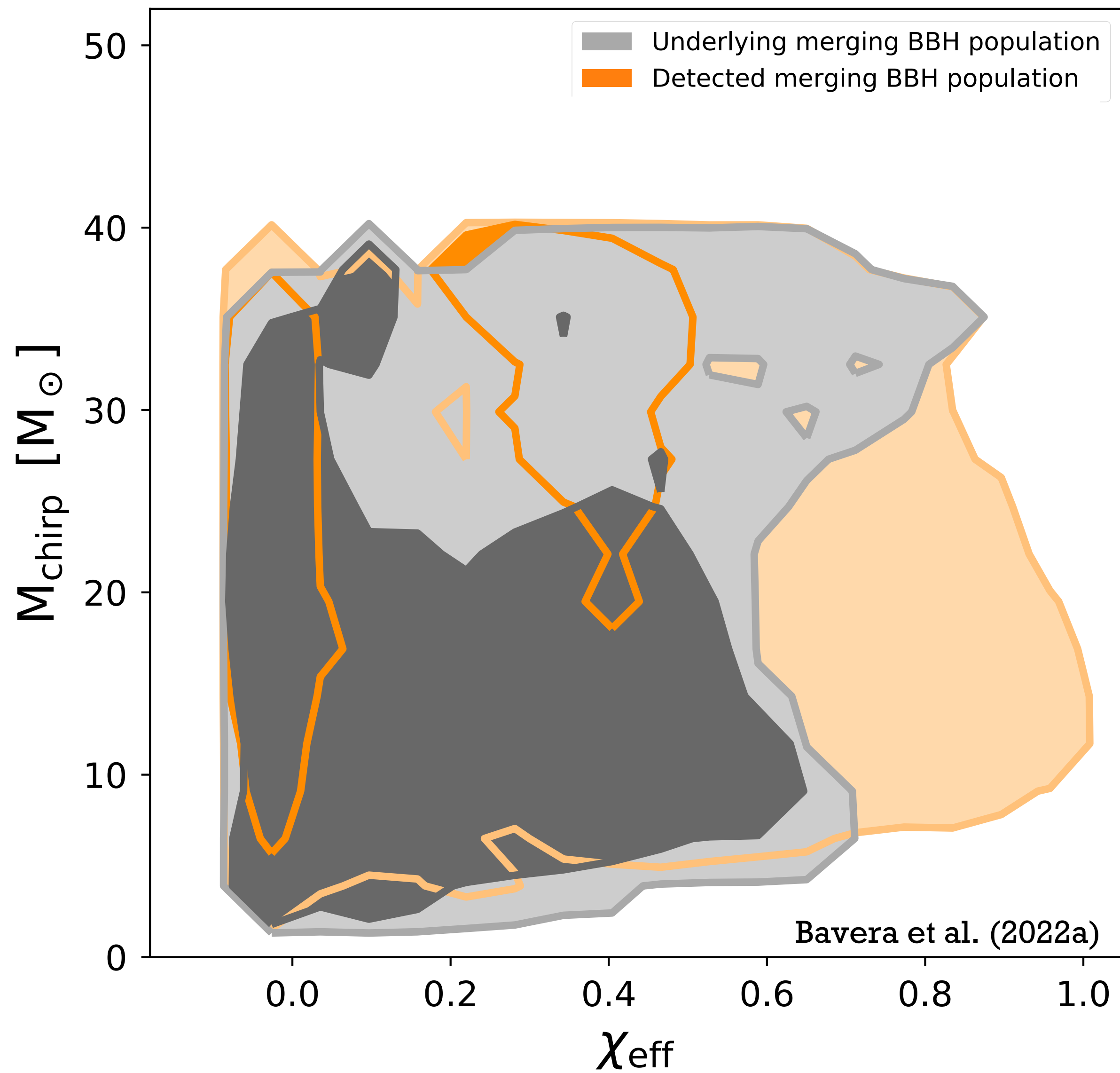
GWTC2



Chirp mass: $M_{\text{chirp}} = \frac{(m_1 m_2)^{3/5}}{(m_1 + m_2)^{1/5}}$

Effective spin parameter: $\chi_{\text{eff}} = \frac{m_1 \vec{\chi}_1 + m_2 \vec{\chi}_2}{m_1 + m_2} \cdot \hat{L}$

Binary black hole mass-spin distribution

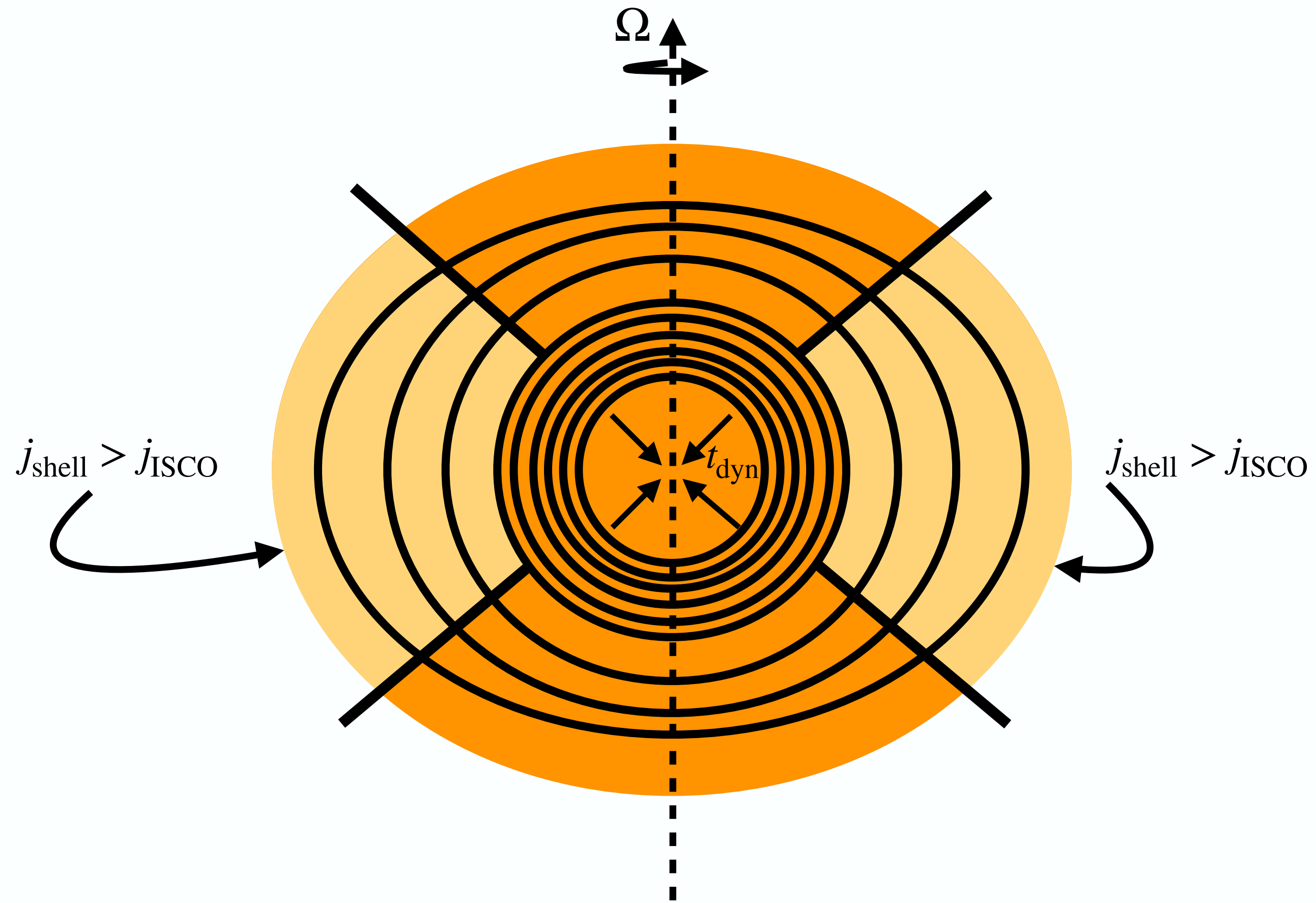


Chirp mass: $M_{\text{chirp}} = \frac{(m_1 m_2)^{3/5}}{(m_1 + m_2)^{1/5}}$

Effective spin parameter: $\chi_{\text{eff}} = \frac{m_1 \vec{\chi}_1 + m_2 \vec{\chi}_2 \cdot \hat{L}}{m_1 + m_2}$

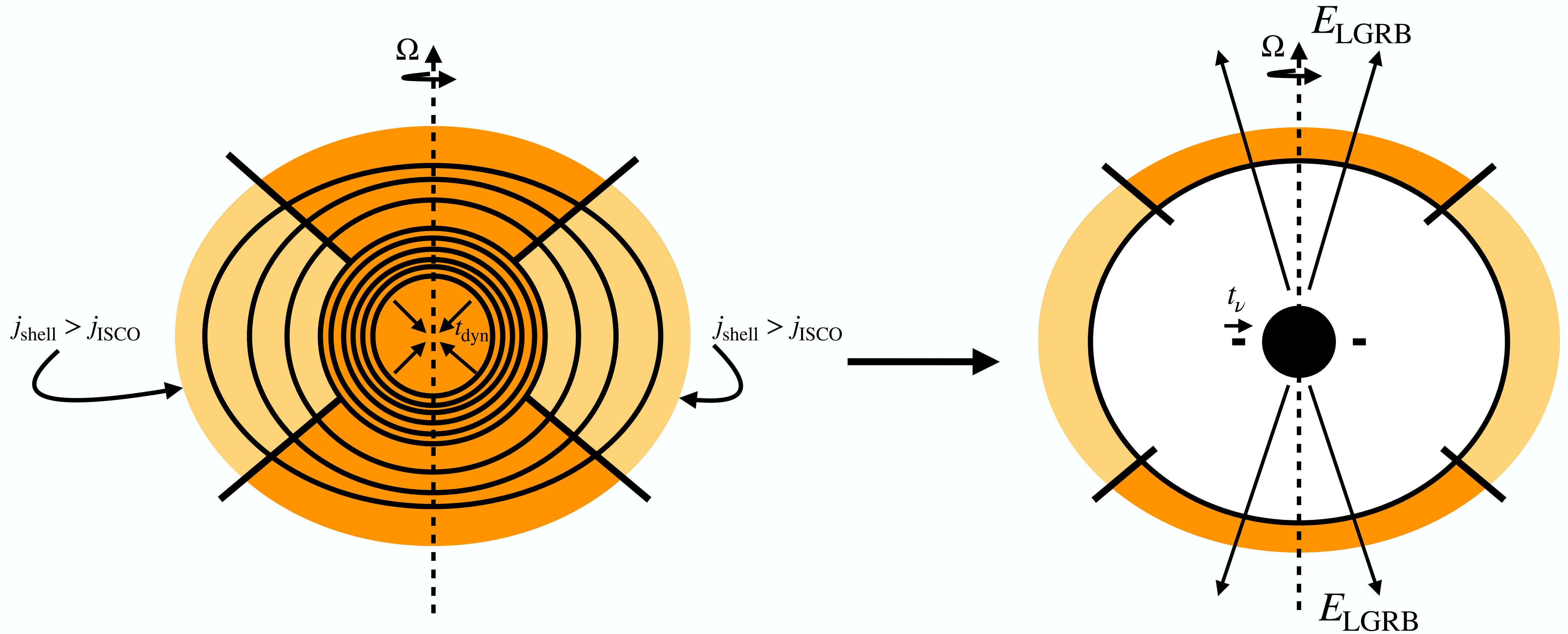
The collapsar model

e.g., Woosley (1993), Paczynski (1998)

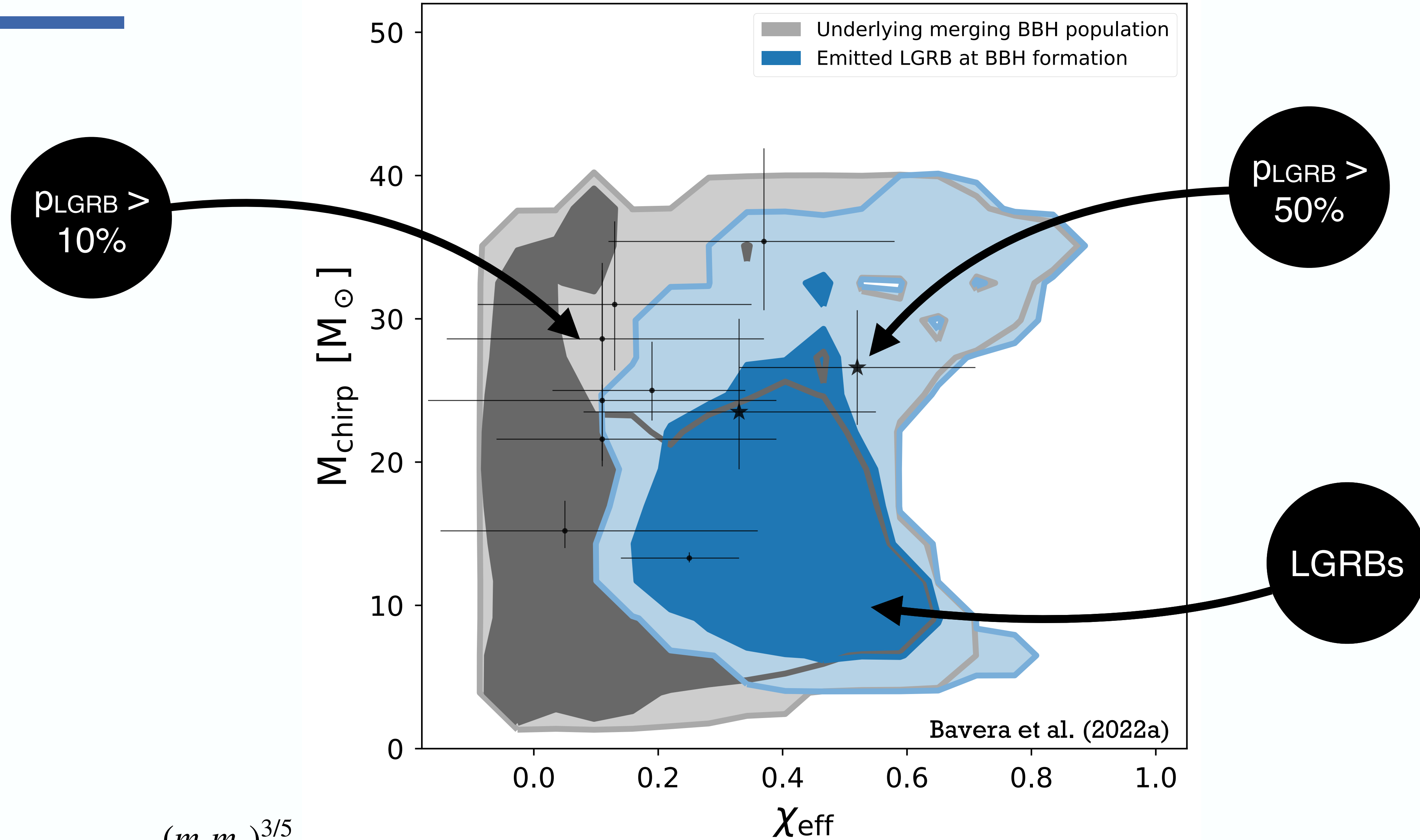


The collapsar model

e.g., Woosley (1993), Paczynski (1998)



Probing binary black hole formation with LGRBs



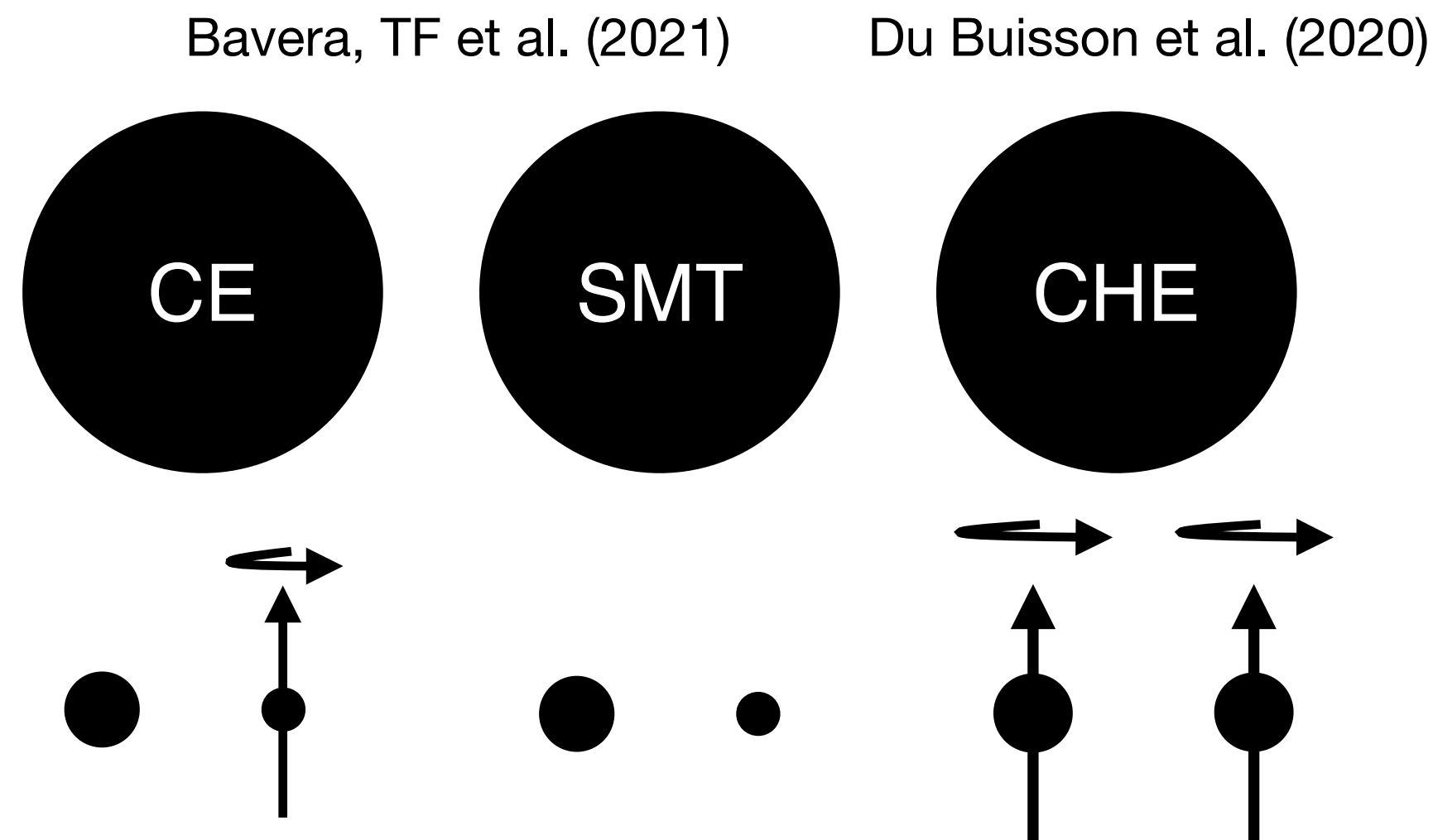
Chirp mass: $M_{\text{chirp}} = \frac{(m_1 m_2)^{3/5}}{(m_1 + m_2)^{1/5}}$

Effective spin parameter: $\chi_{\text{eff}} = \frac{m_1 \vec{\chi}_1 + m_2 \vec{\chi}_2}{m_1 + m_2} \cdot \hat{L}$

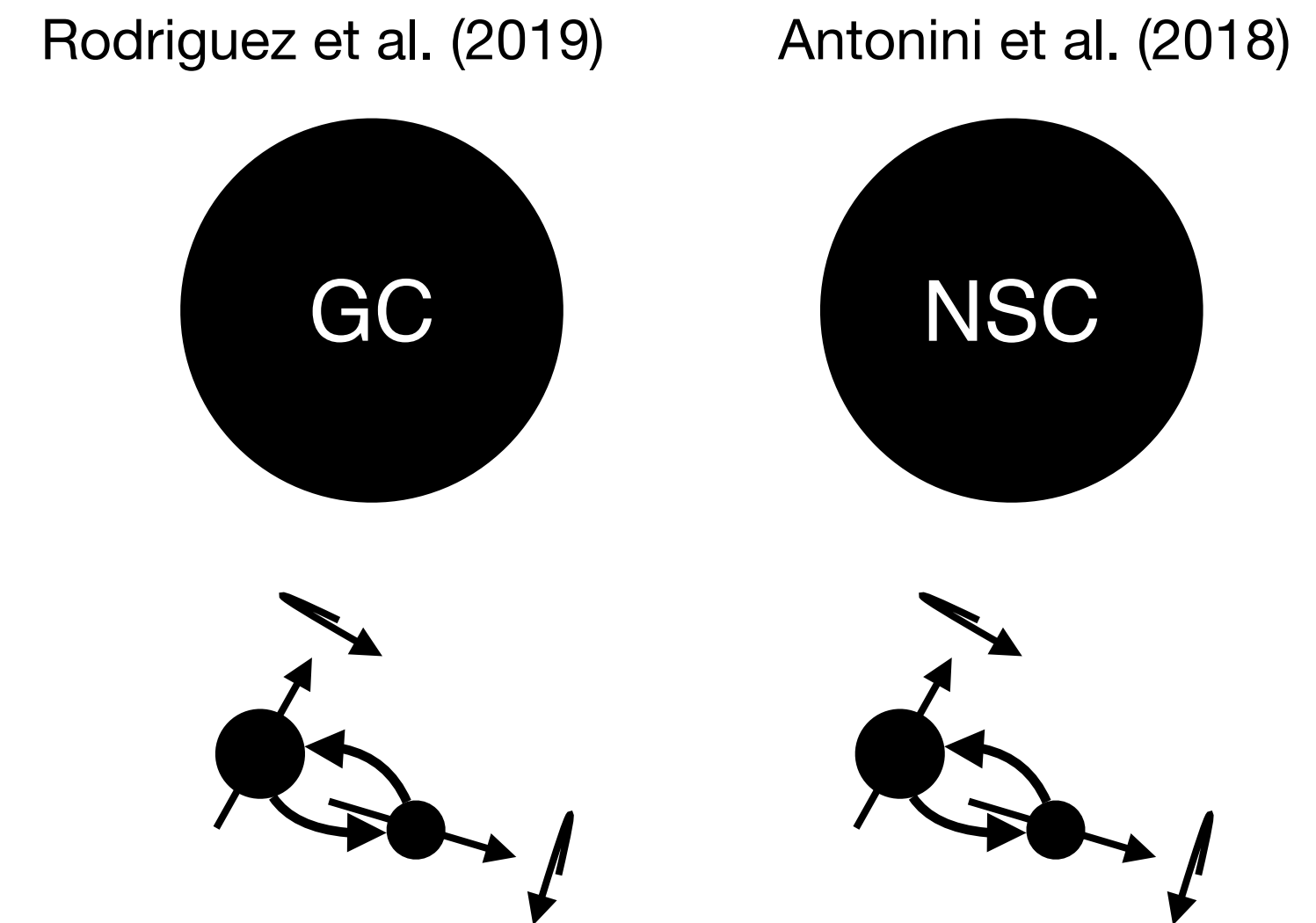
Hierarchical bayesian model selection

e.g. Zevin, Bavera, ..., TF et al. (2021), Wong et al. (2021), Franciolini et al. (2022), Mapelli et al. (2022), Arca Sedda et al. (2023)

Isolated binary evolution



Dynamical formation

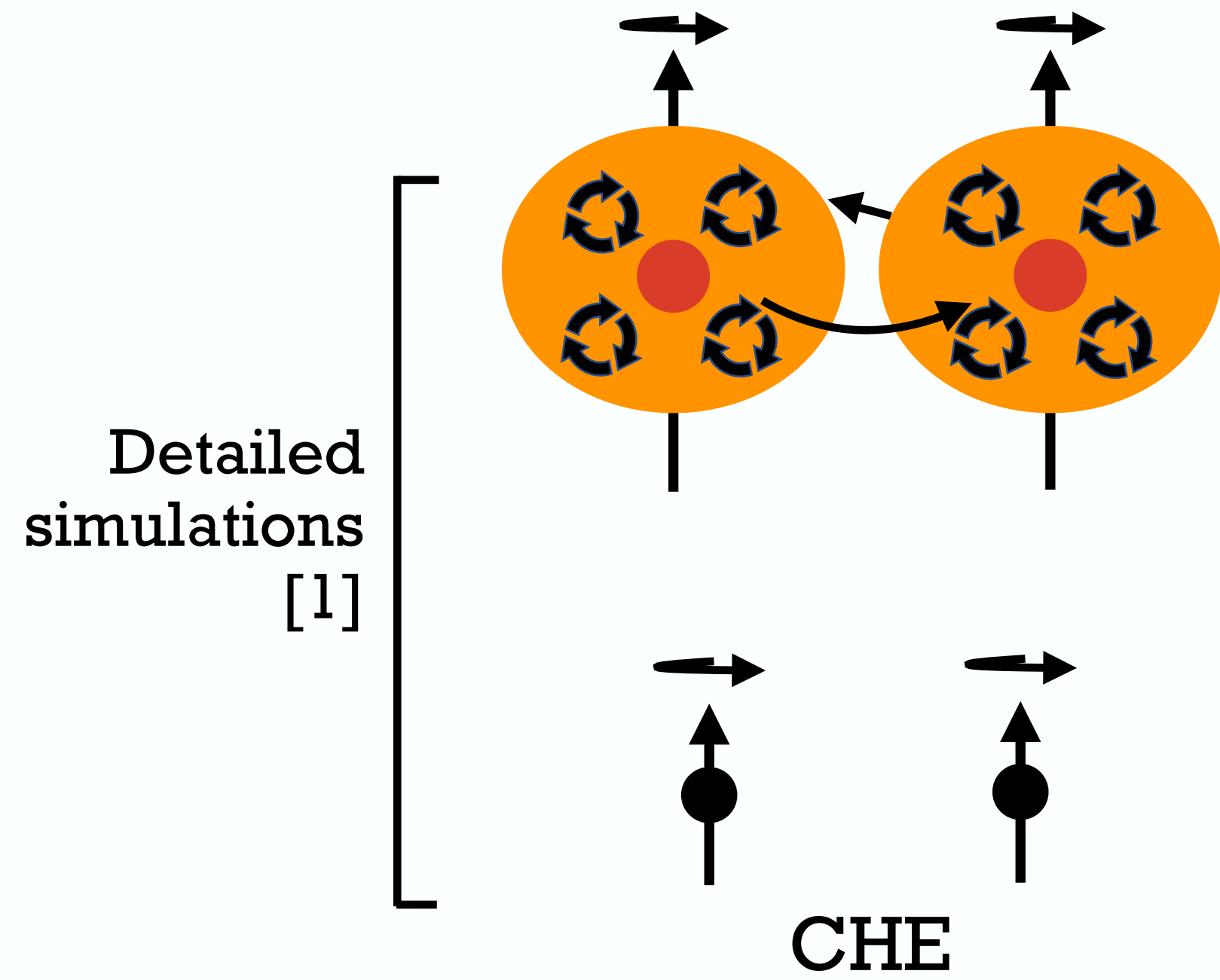


- Constrain uncertain physical processes: e.g., black hole birth spin $|\vec{\chi}|$
- Determine the branching fraction β of each channel

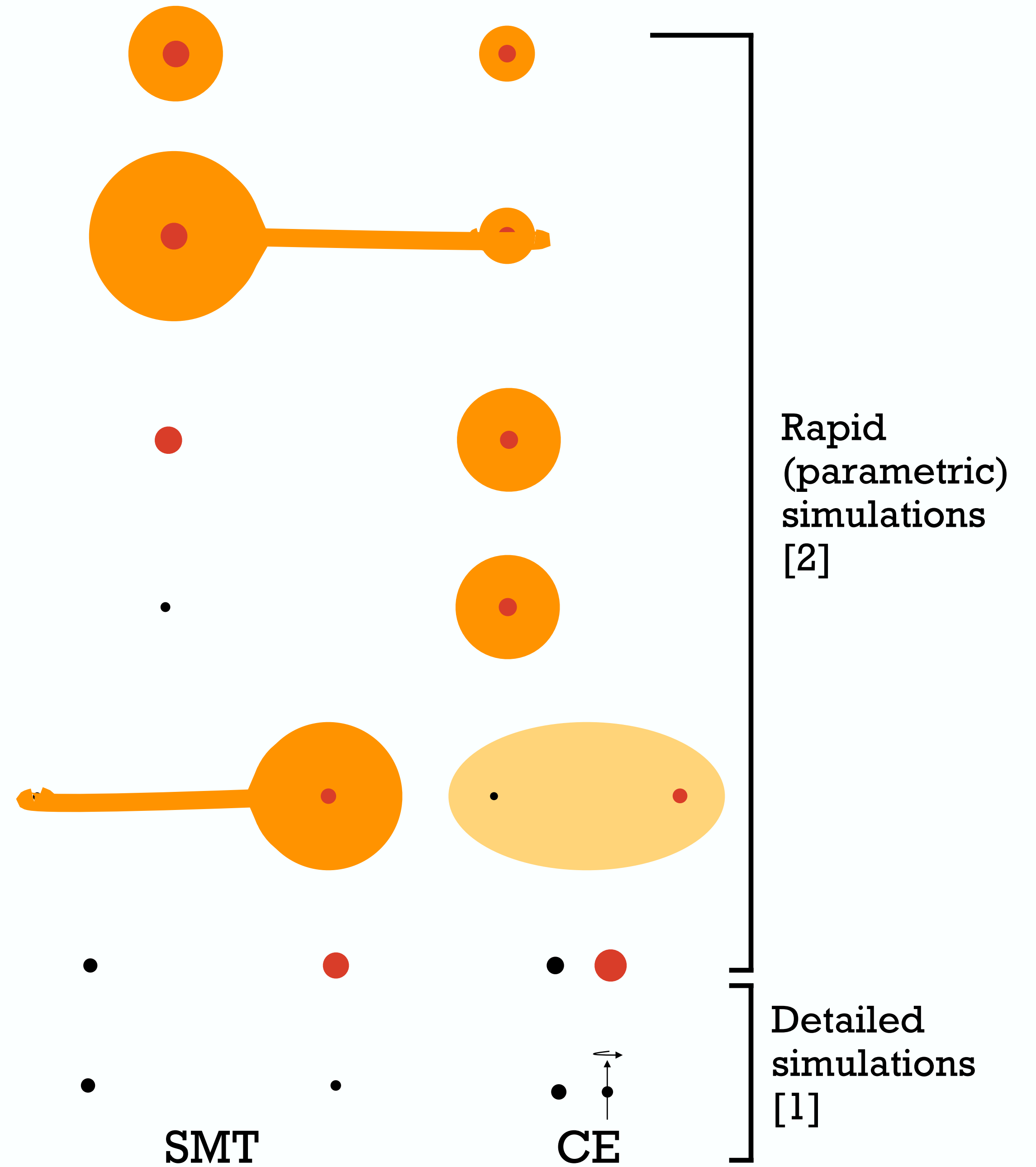
A significant increase in the observed sample and advances in theoretical models* are required for robust results.

*See <https://posydon.org> for one of the efforts to improve the physical accuracy of population synthesis simulations

Binary population synthesis



du Buisson et al. (2021)



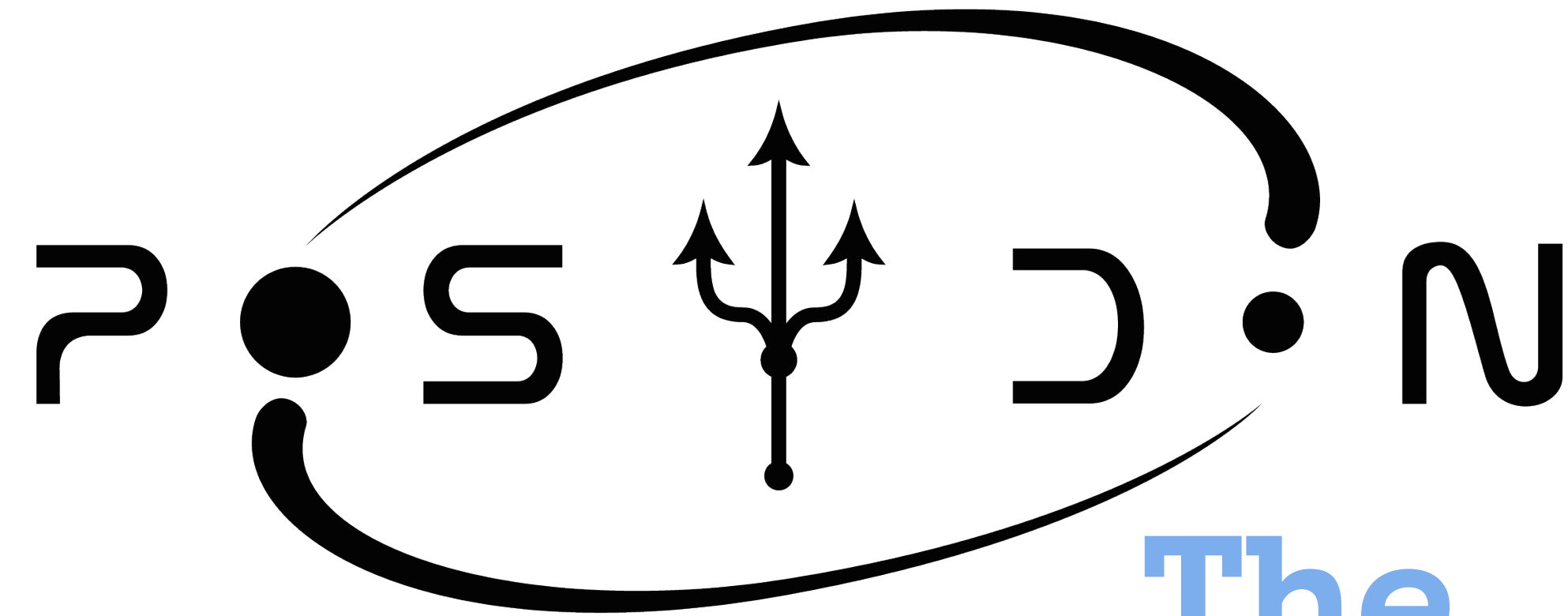
Bavera et al. (2020, 2021a, 2022b,c)



[1] Paxton et al. (2009, 2013, 2015, 2017, 2019)



[2] Breivik et al. (2019)



<https://posydon.org>

POSYDON is a new framework for binary population synthesis studies that uses detailed stellar structure and binary evolution simulations (Fragos et al. 2023).

The core developer team



The **POSYDON** collaboration: Jeff Andrews, Simone Bavera, Christopher Berry, Scott Coughlin, Aaron Dotter, Tassos Fragos, Prabin Giri, Vicky Kalogera, Aggelos Katsaggelos, Konstantinos Kovelakas, Shamal Lalvani, Devina Misra, Philipp Shrivastava, Ying Qin, Jaime Román-Garza, Kyle Rocha, Juan Gabriel Serra Pérez, Petter Alexander Stahle, Meng Sung, Xu Teng, Goce Trajcevski, Zepei Xing, Manos Zapartas



**UNIVERSITÉ
DE GENÈVE**



FONDS NATIONAL SUISSE
SCHWEIZERISCHER NATIONALFONDS
FONDO NAZIONALE SVIZZERO
SWISS NATIONAL SCIENCE FOUNDATION

GORDON AND BETTY
MOORE
FOUNDATION



**NORTHWESTERN
UNIVERSITY**

C I E R A
CENTER FOR INTERDISCIPLINARY EXPLORATION
AND RESEARCH IN ASTROPHYSICS

Key points of this talk

Black hole spins contain the most information regarding the astrophysical origin of BBHs

Correlations of GW observables contain signatures of the astrophysical processes taking place in the formation of BBHs

Approximate progenitor models are reaching the limit of their applicability to GW data interpretation

Moving forward requires constraining astrophysical models with diverse, multi messenger datasets